Influence of initial soil moisture in a Regional Climate Model study over West Africa. Part 1: Impact on the climate mean

Brahima KONÉ[1], Arona DIEDHIOU[1, 2], Adama Diawara[1], Sandrine Anquetin[2], N'datchoh Evelyne Touré[1], Adama Bamba[1], and Arsene Toka Kobea[1]

[1]LASMES - African Centre of Excellence on Climate Change, Biodiversity and Sustainable Agriculture (ACE CCBAD) / Université Félix Houphouët Boigny, Abidjan, Côte d'Ivoire

[2]Univ. Grenoble Alpes, IRD, CNRS, Grenoble INP, IGE, F-38000 Grenoble, France

Correspondence to: Arona DIEDHIOU (arona.diedhiou@ird.fr)

Abstract.

The impact of soil moisture initial conditions on the mean climate over West Africa was examined using the latest version of the Regional Climate Model of the International Centre for Theoretical Physics (RegCM4) at a horizontal resolution of 25 km × 25 km. The soil moisture reanalysis of the European Centre Meteorological Weather Forecast's reanalysis of the 20th century ERA20C is used to initialize the control experiment, while its minimum and maximum values over the entire domain are used to establish the initial dry and wet soil moisture conditions respectively (hereafter dry and wet experiments). For the control, the wet and dry experiments, an ensemble of five runs from June to September are performed. In each experiment, we analyzed the two idealized simulations most sensitive to the dry and wet soil moisture initial conditions. The impact of soil moisture initial conditions on precipitation in West Africa is linear over the Central and West Sahel where dry (wet) experiments lead to rainfall decrease (increase). The strongest precipitation increase is found over the West Sahel for wet experiments with a maximum change value of approximately 40%, while the strongest precipitation decrease is found for dry experiments over Central Sahel with a peak of change of approximately −4%. The sensitivity of soil moisture initial condition can persist for three to four months (90-120 days) depending on the region. However, the influence on precipitation is no longer than one month (between 15 and 30 days). The strongest temperature decrease is located over the Central and West Sahel with a maximum change of approximately −1.5 °C in wet experiments, while the strongest temperature increase is found over the Guinea Coast and Central Sahel for the dry experiments, with a maximum of change around 0.6°C. A significant

33   impact of soil moisture initial conditions on the surface energy fluxes is noted: in the wet (dry)

34   experiments, a cooling (warming) of surface temperature is associated with a decrease (increase)

35   of sensible heat flux, an increase (decrease) of latent heat flux and a decrease (increase) of the

36   boundary layer depth. Part II of this study investigates the influence of soil moisture initial

37   conditions on climate extremes.

38   **1 Introduction**

39   In the climate system, soil moisture is a crucial variable that influences water balance and

40   surface energy components through latent surface fluxes and evaporation. Therefore, soil

41   moisture impacts the development of weather patterns and precipitation. The strength of soil

42   moisture impacts on land-atmosphere coupling varies with location and season. Koster et al.

43   (2004) sustained that improving the simulation of the atmospheric response to the slow

44   variations of land and ocean surface conditions may be important for seasonal climate prediction.

45   The atmospheric response to ocean temperature anomalies has been well documented (Diedhiou

46   and Mahfouf 1996; Kirtman et al. 1998; Rasmusson et al.1982). Schär et al. 1999 sustained that

47   the role of soils may be comparable to that of the oceans. The solar energy received by the

48   oceans is stored in summer and used to heat the atmosphere in winter. Conversely, the

49   precipitation received by the soil is stored in winter and the moistening (cooling) is returned to

50   the atmosphere in summer. Through its impact on surface energy fluxes and evaporation, there

51   are many additional impacts on the climate process of soil moisture, such as boundary-layer

52   stability and air temperature (Hong and Pan, 2000; Kim and Hong 2006). Several studies have

53   shown that the anomalies of soil moisture may persist for several weeks or months, however, its

54   impact remains only for a shorter time in the atmosphere, not exceeding few days (Vinnikov and

55   Yeserkepova 1991; Liu et al., 2014). The important role of anomalies in soil moisture in the

56   coupling between land and atmosphere has been shown in several studies, using numerical

57   climate models (Zhang et al., 2011) and observation datasets (Zhang et al., 2008a; Dirmeyer et

58   al., 2006). For instance, over East Asia, Zhang et al., (2011) showed that soil moisture is found

59   to have a much stronger impact on daily maximum temperature variability than on daily mean

60   temperature variability, but generally has small effects on daily minimum temperature, except in

61   the eastern Tibetan Plateau. They showed that soil moisture has a prominent contribution to

62   precipitation variability in many parts of western China.

63

64   West Africa is known to exhibit strong coupling between soil moisture and precipitation (Koster

65   et al., 2004). Several previous studies have been conducted over West Africa on a global scale

using atmospheric general circulation model (AGCMs) to investigate the impact of soil moisture initial conditions on the land-atmosphere coupling (Koster et al., 2004; Douville and al, 2001; Zhang et al., 2008b). However, at local and regional scales, the land-atmosphere coupling studies with AGCMs, present significant uncertainties (Xue et al. 2010). The regional climate models (RCMs) have been used to simulate the impact on interannual climate variability of anomalies in soil moisture (Seneviratne et al. 2006; Zhang et al. 2011). These studies have received a lot of attention due to the increase of climate variability associated with extreme weather events that have greater societal and environmental impacts. In general, these studies have been conducted in Asia, Europe and America (e.g. Seneviratne et al. 2006 for Europe; Zhang et al. 2011 for Asia; Zhang et al. 2008b for America). Overall, the results of these studies showed that during summer, the strong impact of the anomalies of soil moisture in land-atmosphere occurred mainly over the transition zones with a climate between wet and dry regimes, in agreement with Koster et al. (2004). The relevance and extent of this potential feedback are still poorly understood in West Africa.

This study will focus on the influence of soil moisture initial conditions on climate mean. It is based on performance assessment of the Regional Climate model version 4 coupled to the version 4.5 of the Community Land Model (RegCM4-CLM4.5) performed by Koné et al. (2018) where the ability of the model to reproduce the climate mean has been validated. The descriptions of the model and experimental setup used in this study are presented in Section. 2; in the Section 3, the influence of wet and dry soil moisture initial conditions on the subsequent climate mean is analyzed and discussed; and in Section 4 the main conclusions are presented. While this Part I investigates the impacts on the climate mean, the Part II of this article will be focused on the influence of soil moisture initial conditions on climate extremes.

2. Model and experimental design

2.1 Model description and observed datasets

The fourth generation of the Regional Climate Model (RegCM4) of the International Centre for Theoretical Physics (ICTP) is used in this study. Since its release, its physical representations have been continuously developed and implemented. The version used in the present study is RegCM4.7. The MM5 (Grell et al., 1994) non-hydrostatic dynamical core has been ported to RegCM without removing the existing hydrostatic core. The model dynamical core used in this study is non-hydrostatic. RegCM4 is a limited area model using a sigma pressure vertical grid and the finite differencing algorithm of Arakawa B-grid (Giorgi et al., 2012). The radiation scheme used in this version of RegCM4.7 is derived from the National Center for Atmospheric

99 Research (NCAR) Community Climate Model Version three (CCM3) (Kiehl et al., 1996).

100 Aerosols representation is from Zakey et al. (2006) and Solmon et al. (2006). The large-scale

101 precipitation scheme is from Pal et al. (2000) and the moisture scheme is the SUBgrid EXplicit

102 moisture scheme (SUBEX). The SUBEX take into account the sub-grid scale cloud variability,

103 and the accretion processes and evaporation for stable precipitation following the work of

104 Sundqvist et al., 1989. In the planetary boundary layer (PBL), the sensible heat over ocean and

105 land, water vapour and turbulent transport of momentum are calculated according to the

106 scheme of Holtslag et al. (1990). Heat and moisture, the momentum fluxes of ocean surfaces in

107 this study are computed as in Zeng et al. (1998). In RegCM4.7, convective precipitation and

108 land surface processes can be described by several parameterizations. Based on Koné et al.

109 (2018), we selected the convective scheme reported by Emanuel (1991) and the interaction

110 processes between soil, vegetation and atmosphere are parameterized with CLM4.5. In each

111 grid cell, CLM4.5 has 16 different Plant Functional Types (PFTs) and 10 soil layers (Lawrence

112 et al., 2011; Wang et al., 2016). RegCM4 is integrated over the domain of West Africa depicted

113 in Fig. 1 with 25 km (182x114 grid points; from 20° W-20° E and 5° S-21° N) with horizontal

114 resolution and with 18 vertical levels and the initial and boundary conditions are taken from the

115 European Centre for Medium-Range Weather Forecasts reanalysis (EIN75; Uppala et al., 2008;

116 Simmons et al., 2007). The sea surface temperatures are obtained from the National Oceanic

117 and Atmosphere Administration (NOAA) optimal interpolation weekly (OI_WK) (Reynolds et

118 al., 1996). The topography data are taken from the States Geological Survey (USGS) Global

119 Multi-resolution Terrain Elevation Data (GMTED; Danielson et al., 2011) at 30 arc-second

120 spatial resolution, which is an update to the Global Land Cover Characterization (GTOPO;

121 Loveland et al., 2000) dataset.

122 Our analysis focuses on precipitation and the 2 m air temperature over the West African domain

123 during the June-July-August-September (JJAS). We validate the simulated precipitation with the

124 dataset from the Climate Hazards Group Infrared Precipitation with Stations (CHIRPS)

125 developed at the University of California at Santa Barbara at the 0.05° high-resolution available

126 from 1981 to 2020 (Funk et al., 2015). The validation of the simulated 2 m temperature relies on

127 the CRU datasets (Climate Research Unit version 3.20) from the University of East Anglia,

128 gridded at a horizontal resolution of 0.5° for 1901 to 2011 (Harris et al., 2013). To facilitate

129 comparison between RegCM4 simulations, all products has been re-gridded to 0.22° × 0.22°

130 using a bilinear interpolation method (Nikulin et al., 2012).

131 **2.2 Experiments setup and analysis methodology**

132 The European 20th Century Weather Prediction Center ERA20C soil moisture reanalysis is used

133 to initialize the control experiment, while its domain-wide minimum and maximum values are

134 used to establish the initial dry and wet soil moisture conditions respectively (hereafter dry and

135 wet experiments). We initialized the dry and wet soil moisture initial conditions (in volumetric

136 fraction $m^3.m^{-3}$) respectively at the minimum value ($=0.117*10^{-4}$) and the maximum value

137 ($=0.489$).

138 We designed three experiments (reference, wet, and dry), each with an ensemble of five (5)

139 simulations. The simulation time period for each experiment lasts for 4 months, starting from

140 June 1st to September 30th. The difference between these three experiments is the change in the

141 initial soil moisture condition (reference initial soil moisture condition, wet initial soil moisture

142 condition, and dry initial soil moisture condition) during the first day of the simulation (June 1 st

143 2001, 2002, 2003, 2004 and 2005) over the West African domain. Then, we selected the two

144 runs most impacted by the wet and dry soil moisture initial conditions in order to exhibit the

145 effects on the climate mean beyond the limits of the impacts of RegCM4 initial soil moisture

146 internal forcing. In the same context, several previous studies have selected two extreme years to

147 investigate the climate models sensitivity to soil moisture initial conditions (Hong et al., 2000;

148 Kim and Hong, 2006) outside Africa.

149 Hong and al. (2000) used only two years (three months per year) to investigate the impact of

150 initial soil moisture over North America (in the Great Plains) during two summers spanning

151 May-June-July (MJJ) in 1988 (corresponding to a drought) and 1993 (corresponding to a

152 flooding event). Kim and Hong (2006) selected two contrasting years 1997 (below normal

153 precipitation) and 1998 (above normal precipitation year) for their study over east Asia. The first

154 seven days (Kang et al., 2014) are excluded from the analysis as a spin-up period. Except the

155 geographical location, the experimental setup is the same as that of Hong and Pan (2000). The

156 geographical location of this study is the same as in Koné et al. (2018), with four sub-regions

157 (Fig. 1) exhibiting different features of the annual precipitation cycle: Central Sahel (10° W - 10°

158 E; 10° N - 16° N), West Sahel (18° W - 10° W, 10° N - 16° N), and Guinea Coast (15° W - 10°

159 E; 3° N - 10° N).

160 In several previous studies (Liu et al., 2014; Hong and Pan, 2000; Kim and Hong, 2006), the

161 mean biases (MB) averaged over their studied domains are used to quantify the impact of the soil

162 moisture initial conditions. In our study, we used the MB and the probability density function

163 (PDF; Gao et al., 2016; Jaeger and Seneviratne, 2011) by fitting a normal distribution to better

164 capture how many grid points are impacted by soil moisture initial conditions. The pattern

165 correlation coefficient (PCC) is also used as a spatial correlation to reveal the degree of large-

scale similarity between model simulations and observations. These performance metrics (MB, PCC, and PDF) are computed for both modeled and observed temperature and precipitation only over land grid points.

For the two years most sensitive to soil moisture initial conditions, the Student t-test is used to compare the significance of the difference between a wet or dry sensitivity test (sample 1) and the control (sample 2) in assuming that our two samples are independent and in considering that this method performs well for climate simulations compared to more sophisticated techniques developed to address autocorrelation (Damien et al., 2014). The Student t-test is extensively used for analysis in climate sciences; it is fairly robust and easy to use and interpret (Menedez et al., 2019; Talahashi and Polcher, 2019). The Student t-test takes into account, the difference between the means of each sample, the variance (S) and the number of degrees of freedom ($n - 1$), which depends on the sample size (n). The test statistic is calculated as:

$$t = \frac{\overline{X}_1 - \overline{X}_2}{\sqrt{\dfrac{S_1^2}{n_1} + \dfrac{S_2^2}{n_2}}}$$

Where $\overline{X}_1$ ($\overline{X}_2$) are the sample means, n_1 (n_2) are the sample sizes and S_1^2 (S_2^2) are the sample variances. In this study, the t-test at the 95% confidence level is used to consider statistically significant.

3. Results and discussion

3.1. Influence of soil moisture initial conditions on precipitation.

To identify the two runs most impacted by the dry and wet experiments among the ensemble of five simulations (initiated on 1st June 2001, 2002, 2003, 2004 and 2005), we superimposed on Figure 2, the magnitude of daily soil moisture changes of the 5 runs compared to their corresponding control experiment over West African domain. Figure 2 shows that for the dry experiments (negative values of daily soil moisture changes), the weakest and strongest impacts of soil moisture initial conditions are found with the runs initiated on 1st June 2004 and 2003 respectively. For the wet experiments (positive values of daily soil moisture changes), the weakest impact is found for the run initiated on 1st June 2003, while the other runs exhibit quite the same strong sensitivity. From these results, we selected the two runs initiated on June 1st, 2003 and June 1st, 2004 as the simulations most influenced by the initial wet and dry soil moisture conditions, respectively, to better highlight the effects on the climate mean beyond the

limits of the impact of the initial internal soil moisture forcing. It is worth noting that 2003 is wetter than 2004 and is more sensitive to the dry experiment. While 2004 which is drier than 2003 is more sensitive to the wet experiment.

Figure 3 displays the spatial distribution of the observed mean rainfall (mm/day) from CHIRPS (Fig. 3a, c) for the runs JJAS 2003 and JJAS 2004 and the simulated from control experiments (Fig. 3b, d) initialized with reanalysis soil moisture ERA20C. Table 1 reports the MB and PCC for model simulation compared to CHIRPS, computed for the Central Sahel, Guinea Coast, West Sahel, and the entire West African domain. The CHIRPS product displays a zonal band of rainfall centered around 10° N, decreasing from North to South (Fig. 3a, c). The maximum values are located over the mountain regions of Cameroun and Guinea. While the precipitation minimum values are found over the Sahel and the Sahara. The control experiments (Fig. 3 b and d) reproduced the large-scale pattern of observed rainfall with PCC = 0.72 and 0.77 for the runs JJAS 2003 and JJAS 2004, respectively (Table 1). The spatial extent of rainfall maxima and the North-South gradient are well captured by control experiments; however, their magnitudes are underestimated with respected to the CHIRPS observation. Over West African domain, dry MB reaching −49.31% and −50.56% are obtained for the runs JJAS 2003 and JJAS 2004, respectively (Table 1). Fig. 4 displays the change in mean precipitation (in %) in JJAS 2003 and JJAS 2004 for dry and wet experiments with respect to the control experiments. The dotted area shows changes with a statistical significance of 95%.

Dry and wet sensitivity experiments showed that precipitation is significantly affected by soil moisture initial conditions at magnitude varying with the sub-regions (Fig. 4). Over the Central Sahel, for the dry experiments (Fig. 4a, c), we found a precipitation decrease for JJAS 2003 and JJAS 2004 (Fig. 4a, c). On the other hand, over the Guinea coast, we found an increase in rainfall for both JJAS 2003 and JJAS 2004. For the wet experiments (Fig.4b, d), there is an increase of rainfall over most of studied domains for both JJAS 2003 and JJAS 2004. Overall, the impact of the soil moisture initial conditions on the precipitation is linear only over the Central Sahel for both JJAS 2003 and 2004. Therefore, the dry (wet) experiments exhibits significant decrease (increase) in precipitations with respect to the control experiments (Fig.4a, c).

For a better quantitative evaluation, the PDF distributions of precipitation changes in JJAS 2003 and JJAS 2004, over (a) central Sahel, (b) west Sahel, (c) Guinea coast and (d) West Africa obtained from dry and wet experiments with respect to the control experiments are shown in Fig.

231 5. Table 2 summarizes the maximum values of changes obtained from the PDF's of the different

232 variables used in this study. The impact on precipitation of the soil moisture initial conditions is

233 linear only over Central Sahel (Fig.5a) where the change in dry (wet) experiments showed a

234 precipitation decrease (increase). The strongest precipitation increase is found over West Sahel

235 for the wet experiment with maximum change reached 40%. However, the strongest

236 precipitation decrease is found over the Central Sahel for dry experiment with a maximum

237 change value about −4% (Table 2). We noted that the impacts on precipitation of the wet

238 experiments are greater than those from dry experiments (Table 2). These results are consistent

239 with previous studies that supported a strong relationship between precipitation and soil moisture

240 in particular over the transition zones with a climate between wet and dry climate regimes

241 (Koster et al., 2004; Liu et al., 2014; Douville et al., 2001).

242

243 Fig. 6 and Fig. 7 shows the changes in the daily soil moisture and precipitation, respectively,

244 from dry and wet experiments with respect to the control experiments, during the runs JJAS

245 2003 and JJAS 2004. To compute the changes of daily soil moisture, we considered the second

246 top soil layer in CLM4.5 (from 0 to 2.80 cm). In general, the impacts of soil moisture initial

247 conditions on the daily soil moisture persist from three to four months over the studied domains

248 (Fig.6). The strongest duration and amplitude of the impact on the daily soil moisture is found

249 over the West Sahel sub-region. The impact on the daily soil moisture lasts four months in JJAS

250 2003 and JJAS 2004. For wet experiments, the weakest duration of the impact of soil moisture

251 initial conditions is found over the Guinea Coast and lasts three months (Fig. 6c). While, for dry

252 experiments, the weakest impact on the daily soil moisture is found over Central Sahel and lasted

253 three months (Fig. 6a). These results are in line with previous works which argued that the soil

254 moisture-atmosphere feedback strength and the land memory are place dependent (Vinnikov et

255 al. 1996; Vinnikov and Yeserkepova 1991).

256 Figure 7 shows the changes of the daily precipitation to the soil moisture initial conditions over

257 the different studied domains. The impact of the wet experiments on daily precipitation is greater

258 in magnitude than that of dry experiments over most studied domains (Fig. 7). For dry

259 experiments, the strongest daily precipitation response (about −4mm.day^{-1}), is found over the

260 Guinea Coast in the run JJAS 2003 (Fig. 7c). While for the wet experiments, the strongest impact

261 on the daily precipitation is more than 8mm.day^{-1} and it is found over the West Sahel and the

262 Guinea Coast (Fig. 7b, c, respectively). It is worth to note that the impact of initial soil moisture

263 conditions on daily precipitation is much shorter than the duration of the impact on daily soil

264 moisture. The significant impact on daily precipitation is found only for wet experiments, and

did not last more than 15 days in large parts of the study domain, excepted over wetter sub-region of Guinea Coast where it lasts approximately one month. We noted that the precipitation peaks over West Sahel and Guinea Coast (Fig. 7b and c, respectively) during August and September coincide with fluctuation in the daily soil moisture impact (Fig.6b and c). This probably indicates the strong feedback of soil moisture and precipitation during this period over the Guinea Coast and West Sahel regions.

To investigate the causes of the precipitation changes, we examined the vertical profile change in relative humidity and air temperature for the runs JJAS 2003 and JJAS 2004, respectively, from dry and wet experiments with respect their control experiment.

The impacts on relative humidity and air temperature (Fig.8 and Fig.9, respectively) of soil moisture initial conditions are significant in the lower troposphere. In the low and mid-troposphere, a drying and a warming are found in the dry experiments, while a moistening and a cooling are simulated in the wet experiments. This indicates that a weak (strong) dry convection is found over most of the studied domains for dry (wet) experiments. The strongest impact on the relative humidity and temperature in the lower and middle troposphere is found over central Sahel (Fig.8a and Fig. 9a).

For the upper troposphere, the significant impact on relative humidity and temperature is found only for wet experiments, and exhibited a drying and a warming over most of studied domains (Fig.8 and Fig.9). This impact for the wet experiments was also reported by Hong and Pal (2000).

To understand other causes of the precipitation changes illustrated in Fig. 4, we analyzed the changes in lower tropospheric wind (850hpa) and specific humidity for the runs JJAS 2003 and JJAS 2004 during the dry and wet experiments with respect to the control experiments (Fig. 10). For the dry experiments (Fig. 10a, c), we found that the moistening of the lower atmosphere decreases over most of the study domain. However, the strong wind magnitude changes over the Atlantic Ocean bring the moistening from the ocean to the Guinea Coast and West Sahel. This can explain the precipitation increase over these sub-regions in the dry experiments. Over Central Sahel, the strong decrease in precipitation seems to be associated with the decrease of specific humidity which is particularly notable in the run JJAS 2003 (Fig.4a). Conversely, for the wet experiments (Fig.10b, d), an increase in the moistening of the atmosphere is found mainly over the Sahel band while further South, a decrease of the specific humidity is simulated over Guinea Coast. The strong change in wind magnitude shifts the moistening from the North to the South, leading to precipitation increase over most part of study domain (Fig.4 b and d). These

298   results are broadly consistent with precipitation changes for dry and wet experiments shown in

299   Figure 4.

300   Summarizing these results, the impact of soil moisture initial conditions is linear only over the

301   Central Sahel for the runs JJAS 2003 and 2004. The strongest precipitation decrease is found

302   over Central Sahel for the dry experiment in the run JJAS 2003 with maximum change reaching

303   −4%. While, the strongest precipitation increase is found over the West Sahel for the wet

304   experiment in the run JJAS 2004 with maximum change about 40%. The impact of soil moisture

305   initial conditions on daily soil moisture can persist for three to four months according to the sub-

306   domains, while the significant impact on precipitation (greater than 1mm.day^{-1}) is much shorter

307   and no longer than one month. The impact of soil moisture initial conditions is mostly confined

308   at the near-surface climate and somewhat at the upper troposphere.

309   **3.2. Influence on temperature and other surface fluxes.**

310   Figure 11 shows the spatial distribution of the mean observed 2m temperature from CRU during

311   JJAS 2003 and JJAS 2004 (Fig. 11a, c, respectively) and the mean simulated temperature from

312   the control experiments of runs JJAS 2003 and JJAS 2004 (Fig.11 b, d, respectively) initialized

313   with ERA20C. Table 3 summarizes the PCC and MB between model simulations of temperature

314   with respect to CRU, calculated for the West Sahel, Central Sahel, Guinea Coast and the entire

315   West African domain. The CRU temperature displays a zonal distribution over the whole West

316   Africa domain. Maximum values of approximately 34 °C are found over the Sahara, while the

317   lowest temperatures not exceed 26°C, are located over the Guinea Coast especially in orographic

318   regions such as Guinean highlands, Cameroon Mountains and the Jos Plateau. The control

319   experiments (Fig. 11b, d) showed good agreement in the representation of the large-scale pattern

320   of CRU observation, with PCC about 0.99 for both JJAS 2003 and JJAS 2004 (Table 3),

321   including the meridional gradient between Sahara Desert and Guinea Coast which is crucial for

322   the African Easterly Jet evolution and formation (Thorncroft and Blackburn 1999; Cook 1999).

323   The spatial extent of temperature maxima and minima are well reproduced by control

324   experiments, however their magnitudes are overestimated compared to CRU. The strongest

325   warm MB of control experiments relative to CRU are approximately 2.68 °C and 2.14 °C

326   respectively for JJAS 2003 and JJAS 2004; they are found over the West Sahel (Table 3).

327   Figure 12 shows changes in mean temperature for the runs JJAS 2003 and JJAS 2004 of dry and

328   wet experiments with respect to the control experiments. The dots show areas where impacts of

329   soil moisture initial condition are statistically significant at the 0.05 level. In the dry experiments,

330   for both JJAS 2003 and JJAS 2004 runs, the warmest changes are located under the latitude 13°

N, with maximum values located over the Guinea coast. For the wet experiments, the coolest changes are found over the West and Central Sahel.

For a better quantitative evaluation, the PDF distributions of the changes in mean temperature in runs JJAS 2003 and JJAS 2004 are showed in Figure 13. The impact on temperature is linear over the Central Sahel, Guinea Coast and the whole West African domain (Fig.13a, c and d). The strongest mean temperature decrease is observed over the Central and West Sahel in wet experiments with the maximum change approximately -1.5 °C (Table 2). However, the strongest increase of mean temperature is found over the Central Sahel (JJAS 2003) and the Guinea coast (JJAS 2004) in dry experiments reaching 0.56 °C and 0.59°C, respectively (Table 2). Overall, the impact in the dry (wet) sensitivity experiments on 2m-temperature showed an increase (decrease) in warming (cooling) for both JJAS 2003 and JJAS 2004 over most of the studied domains. The exception is found over the west Sahel, where both dry and wet experiments lead to temperature increase (Fig.13, Table2).

We now analyze the influence of soil moisture initial conditions anomalies on land energy balance, particularly on the surface fluxes sensible and latent heat. Figure 14 shows changes in sensible heat fluxes (in $W.m^{-2}$) in runs JJAS 2003 and JJAS 2004, from dry and wet experiments compared to the control experiments. The dots show changes that are statistically significant at the 0.05 level. As shown in figure 14, the impact on sensible fluxes of soil moisture initial conditions is strong. It is linear over most of the studied domains: the dry (wet) experiments with respect to the control exhibits significant increase (decrease) of the sensible heat (Fig.14).

The PDF distributions of change in sensible heat flux are displayed in Figure 15. The dry (wet) experiments showed an increase (a decrease) of the sensible flux in both runs JJAS 2003 and JJAS 2004 (Fig. 15). The impact in wet experiments is strong over Central and West Sahel compared to the dry experiments, but not for Guinea Coast (Fig. 15, Table 2). In the dry experiments, the strongest sensible heat flux increase is found over Guinea Coast, with maximum change about 9.18 $W.m^{-2}$ during JJAS 2004 (see Table 2). In the wet experiments, the strongest sensible heat flux decrease is located over Central Sahel with maximum change about -39.66 $W.m^{-2}$ during JJAS 2003 (see Table 2).

Unlike the case of sensible heat flux, changes in latent heat showed a linear opposite patterns. Dry experiments result in latent heat flux decrease, while the wet experiments result in latent heat flux increase over most of studied domains (Fig. 16). The PDF distributions of latent heat flux changes are shown in Figure 17. In the wet experiments, the strongest latent heat flux increase is found over West Sahel with maximum change reaching 36.49 $W.m^{-2}$ in JJAS 2004

(Table2). In the dry experiments, the strongest latent heat flux decrease is located over Guinea Coast with maximum change reaching -14.64 W.m^{-2} in JJAS 2004 (Table2). It is worth to note that the impacts on latent and sensible heat flux in wet experiments are stronger compared to those in the dry experiments over most of studied domains, except over Guinea Coast (Table 2).

We then examined the impact on the stability of the PBL of the soil moisture initial conditions. Different spatial distributions of surface fluxes significantly affect the boundary layer development. Soil moisture can influence rainfall by limiting evapotranspiration, which affects the development of the daytime PBL and thereby the initiation and intensity of convective precipitation (Eltahir, 1998). Figure 18 shows changes in PBL (in m) for JJAS 2003 and JJAS 2004, from dry and wet experiments with respect to the control experiments with dotted areas that are statistically significant at the 0.05 level. The soil moisture initial conditions impact significantly the PBL. The dry experiments show PBL increase under the latitude 15 °N for both JJAS 2003 and JJAS 2004 (Fig.18 a and c, respectively). For the wet experiments, a PBL decrease is found over most of the studied domains. The PDF of PBL changes (Fig. 19) show that the impact on PBL is linear over most of studied domains. The dry (wet) experiments lead to an increase (decrease) of PBL for both JJAS 2003 and JJAS 2004. The strongest PBL increase (decrease) is found over Guinea Coast (West Sahel) in dry (wet) experiments during JJAS 2004 (JJAS 2003) reaching 146.80m (-293.23m). A dry (wet) air is located above the areas where PBL increase (decrease), causing the air column to become warm (cool) and dry (moist) for the dry (wet) experiment (see Fig. 8 and Fig. 9). These results are consistent with the work of Hong and Pan (2000).

Summarizing the results of this section, we found that in the wet experiments, the cooling of the mean temperature is associated with an increase of the latent heat flux, a decrease of the sensible heat flux and of the PBL depth over most studied domain. Conversely, in the dry experiments, the warming of surface temperature is associated with a decrease of latent heat, an increase of sensible heat flux and PBL depth.

4. Conclusion

The impact of the soil moisture initial conditions on the subsequent summer (JJAS) mean climate over West Africa was explored using the RegCM4-CLM45. In particular, the aim of this study was to investigate how soil moisture initialization at the beginning of the rainy season may affect the intra-seasonal variability of temperature and precipitation mean within the subsequent season (June to September).

398 For this purpose, we set up three numerical experiments with RegCM4 in which we applied, at

399 the first day (June 1st), a control soil moisture initial condition (control experiment), a wet soil

400 moisture initial condition (wet experiment), and a dry soil moisture initial condition (dry

401 experiment). For each experiment, an ensemble of five simulations beginning from June 1st to

402 September 30th(JJAS), for the years 2001 to 2005 is performed. In this paper, we present results

403 of the two runs JJAS 2003 and JJAS 2004 most impacted by soil moisture dry and wet initial

404 conditions respectively to avoid effects of initial soil moisture internal forcing.

405 The impact of soil moisture initial conditions on precipitation is linear only over the Central

406 Sahel for both JJAS 2003 and JJAS 2004, and over the West Sahel especially in JJAS 2004. In

407 the dry experiment, the strongest precipitation decrease is found over the Central Sahel in JJAS

408 2003 with maximum change reaching −4% while in the wet experiment, the strongest

409 precipitation increase is found over the West Sahel in JJAS 2004 with maximum change

410 reaching 40%. The impact of soil moisture initial conditions can persist for three to four months

411 (90-120 days) depending on the sub-region but the impact on precipitation is no longer than 30

412 days (15 days over the Sahel and 30 days over the Guinea Sahel). This study shows that when

413 averaged over the entire West African region, the sensitivity of rainfall to initial soil moisture

414 conditions is not captured. However, it is important to have a good initialization of soil moisture

415 because depending on the region, the sensitivity of rainfall can be more or less strong. Indeed,

416 rainfall is more sensitive to initial soil moisture conditions in the western and central Sahel (arid

417 zones) than in the Guinean Coast (humid zone). In these arid Sahelian zones, wetter initial

418 conditions will result in more rainfall, especially in the West Sahel, and dry initial conditions

419 will result in less rainfall, especially in the Central Sahel. In the Guinean Coast, the sensitivity of

420 precipitation to initial soil moisture conditions is lower and other factors could be involved such

421 as moisture advection from the Atlantic by the monsoon flow (Koné et al., 2018) and a lower

422 albedo (Charney 1975).

423 Our results show that soil moisture wet initial conditions lead in the lower troposphere to an

424 increase of relative humidity associated with a cooling of air temperature and in the upper

425 troposphere, to a decrease of relative humidity and a warming of air temperature. While the dry

426 experiments mainly impact the lower troposphere with a decrease of the relative humidity

427 associated with a warming air temperature.

428 The temperature at 2m is more sensitive to the anomalies of initial soil moisture condition than

429 the precipitation. The strongest impact on 2m-temperature is found over the Central Sahel with a

430 maximum change about −1.5 °C and 0.6°C for the wet and dry experiments, respectively.

431 Our study showed significant impacts of soil moisture initial conditions on the surface energy

432 fluxes. For the wet experiments, we found that the cooling of surface temperature is associated

433 with a decrease of the sensible heat flux, an increase of the latent heat flux and a decrease of the

434 PBL depth. For the dry experiments, the warming of surface temperature is associated with an

435 increase of the sensible heat flux, a decrease of the latent heat flux and an increase of the PBL

436 depth.

437 This study showed that soil moisture as a boundary condition plays a major role in controlling

438 summer climate variability not only over the Sahel band but also over humid zones such as

439 Guinea Coast. Therefore, the good prescription of soil moisture initial conditions could improve

440 the simulation of precipitation and temperature, which would help to reduce biases in climate

441 model simulations. Overall, land surface initialization can contribute to improving sub-seasonal

442 to seasonal forecast skill, but this requires further investigation.

443 This study is the first investigating the impact of soil moisture initial conditions in West Africa.

444 However, this study is based on idealized experiments: sensitivity experiments such as "wet" and

445 "dry" ones conducted in this study were not intended to simulate real climate since such

446 extremes are very rare. Moreover, this study is very specific to RegCM4. In the future, an

447 investigation using different RCMs in a multi-model framework will contribute to better quantify

448 the impact of soil moisture initial conditions. At shorter timescales, there is a need to understand

449 how the soil moisture initial conditions contribute to the triggering and the maintenance of the

450 mesoscale convective systems which are known to explain large amount of rainfall in the region

451 (Mathon et al., 2002). Finally, in the context of climate change, considering the projected

452 increase of high-impact weather events in the region, there is a need to explore the sensitivity of

453 soil moisture initial conditions to climate extremes.

454

455 **Authors contributions**

456 The authors declare to have no conflict of interest with this work. B. Koné and A. Diedhiou fixed

457 the analysis framework. B. Koné carried out all the simulations and figures production according

458 to the work plan proposed by A. Diedhiou. Figures for this manuscript were prepared by B. Koné

459 according the outline proposed by A. Diedhiou and A. Diawara. All authors contributed to the

460 analyses and to the drafting of this manuscript.

461 **Acknowledgements**

462 The research leading to this publication is co-funded by the NERC/DFID "Future Climate for

463 Africa" programme under the AMMA-2050 project, grant number NE/M019969/1 and by IRD

464 (Institut de Recherche pour le Développement; France) grant number UMR IGE Imputation

465 252RA5.

466

467

468

469 **References:**

470

471 Beljaars A. C. M., Viterbo P., Miller M. J., and Betts A. K.: The anomalous rainfall over the

472 United States during July 1993: Sensitivity to land surface parameterization and soil moisture

473 anomalies, Mon. Weather Rev., 124(3), 362–382, doi:10.1175/1520-0493(1996)124<0362:

474 TAROTU>2.0.CO;2, 1996.

475

476 Bosilovich, M. G., and Sun W. Y.: Numerical simulations of the 1993 Midwestern flood: Land–

477 atmosphere interactions. J. Climate, 12, 1490–1505, 1999.

478

479 Charney, J. G. Dynamics of deserts and drought in the Sahel. Quarterly Journal of the Royal

480 Meteorological Society, 101(428), 193-202. https://doi-org/10.1002/qj.49710142802, 1975.

481

482 Cook K. H.: Generation of the African easterly jet and its role in determining West African

483 precipitation, J. Climate, 12, 1165–1184, https://doi.org/10.1175/1520-0442(1999)012

484 <1165:GOTAEJ> 2.0.CO;2, 1999.

485

486 Damien Decremer, Chul E. Chung, Annica M. L. Ekman & Jenny Brandefelt (2014) Which

487 significance test performs the best in climate simulations?, Tellus A: Dynamic Meteorology and

488 Oceanography, 66:1, DOI: 10.3402/tellusa.v66.23139.

489

490 Danielson J.J., and Gesch D.B.: Global multi-resolution terrain elevation data 2010

491 (GMTED2010): U.S. Geological Survey Open-File Report 2011–1073, 26 p, 2011.

492

493 Diedhiou, A., & Mahfouf, J. F. Comparative influence of land and sea surfaces on the Sahelian

494 drought: a numerical study. In Annales Geophysicae (Vol. 14, No. 1, pp. 115-130). Copernicus

495 GmbH, https://doi.org/10.1007/s00585-996-0115-6. 1996.

496

497 Dirmeyer P. A., Koster R. D., and Guo Z.: Do global models properly represent the feedback

498 between land and atmosphere, J. Hydrometeorol., 7(6), 1177–1198, doi:10.1175/JHM532.1,

499 2006.

500

501 Douville, F. Chauvin, and H. Broqua.: Influence of soil moisture on the Asian and African

502 monsoons. Part I: Mean monsoon and daily precipitation. J. Climate, 14, 2381–2403, 2001.

503

504 Eltahir E. A. B.: A soil moisture-rainfall feedback mechanism 1. Theory and observations, Water

505 Resour. Res., 34, 765–776, doi:10.1029/97WR03499, 1998.

506

507 Emanuel K. A.: A scheme for representing cumulus convection in large-scale models. Journal of

508 the Atmospheric Science 48: 2313–2335, 1991.

509

510 Funk, C., Peterson, P., Landsfeld, M. et al. The climate hazards infrared precipitation with

511 stations—a new environmental record for monitoring extremes. Sci Data 2, 150066 (2015).

512 https://doi.org/10.1038/sdata.2015.66

513

514 Gao, X.-J., Shi, Y., and Giorgi, F.: Comparison of convective parameterizations in RegCM4

515 experiments over China with CLM as the land surface model, Atmos. Ocean. Sci. Lett., 9, 246–

516 254, https://doi.org/10.1080/16742834.2016.1172938, 2016.

517

518 Giorgi F., Coppola E., Solmon F., Mariotti L., Sylla M. B., Bi X., Elguindi N., Diro G. T., Nair

519 V., Giuliani G., Cozzini S., Guettler I., O'Brien T., Tawfik A., Shalaby A., Zakey A. S., Steiner

520 A., Stordal F., Sloan L., and Brankovic C.: RegCM4: model description and preliminary tests

521 over multiple CORDEX domains, Clim. Res., 52, 7–29, https://doi.org/10.3354/cr01018, 2012.

522

523 Grell G., Dudhia J. and Stauffer D. R.: A description of the fifth generation Penn State/NCAR

524 Mesoscale Model (MM5), National Center for Atmospheric Research Tech Note NCAR/TN-

525 398+STR, NCAR, Boulder, CO, 1994.

526

527 Harris I., Jones P. D., Osborn T. J. and Lister D. H.: Updated high-resolution grids of monthly

528 climatic observations, Int. J. Climatol., 34, 623–642, https://doi.org/10.1002/joc.3711, 2013.

Holtslag A., De Bruijn E., and Pan H. L.: A high resolution air mass transformation model for short-range weather forecasting, Mon. Weather Rev., 118, 1561–1575, 1990.

Hong S-Y. and Pan H-L.: Impact of soil moisture anomalies on seasonal, summertime circulation over North America in a regional climate model. J. Geophys. Res., 105 (D24), 29 625–29 634, 2000.

Jaeger E. B., and Seneviratne S.I.: Impact of soil moisture-atmosphere coupling on European climate extremes and trends in a regional climate model, Clim. Dyn., 36(9-10), 1919-1939, doi:10.1007/s00382-010-0780-8, 2011.

Kang S, Im E.-S. and Ahn J.-B.: The impact of two land-surface schemes on the characteristics of summer precipitation over East Asia from the RegCM4 simulations Int. J. Climatol. 34: 3986-3997, 2014.

Kiehl J., Hack J., Bonan G., Boville B., Breigleb B., Williamson D., Rasch P.; Description of the NCAR Community Climate Model (CCM3). National Center for Atmospheric Research Tech Note NCAR/TN-420+STR, NCAR, Boulder, CO, 1996.

Kim J-E., and Hong S-Y.: Impact of Soil Moisture Anomalies on Summer Rainfall over East Asia: A Regional Climate Model Study, Journal of Climate. Vol. 20, 5732–5743, DOI: 10.1175/2006JCLI1358.1, 2006.

Kirtman B.P., Schopf P. S.: Decadal Variability in ENSO Predictability and Prediction. Journal of Clim. 11, 2804, 1998.

Koné B., Diedhiou A., N'datchoh E. T., Sylla M. B., Giorgi F., Anquetin S., Bamba A., Diawara A., and Kobea A. T.: Sensitivity study of the regional climate model RegCM4 to different convective schemes over West Africa. Earth Syst. Dynam., 9, 1261–1278. https://doi.org/10.5194/esd-9-1261-2018, 2018.

Koster R. D., Dirmeyer P. A., Zhichang G., Bonan G., Chan E., Cox P., Gordon C. T., Kanae S., Kowalczyk E., Lawrence D., Liu P., Lu C. H, Malyshev S., McAvaney B., Mitchell K, Mocko

D., Oki T., Oleson K., Pitman A., Sud Y. C., Taylor C. M., Verseghy D., Vasic R., Xue Y., Yamada T.: Regions of strong coupling between soil moisture and precipitation, Science, 305, 1138–1140, doi:10.1126/science.1100217, 2004.

Lawrence D.M., Oleson K.W., Flanner M.G., Thornton P.E., Swenson S.C., Lawrence P.J., Zeng X., Yang Z.-L., Levis S., Sakaguchi K., Bonan G.B., and Slater A.G.:Parameterization improvements and functional and structuraladvances in version 4 of the Community Land Model. J. Adv. Model. Earth Sys. 3. DOI:10.1029/2011MS000045, 2011.

Liu D., WangG. L., Mei R., Yu Z. B. and Gu H. H.: Diagnosing the strength of land-atmosphere coupling at sub-seasonal to seasonal time scales in Asia, J. Hydrometeor., doi:10.1175/JHM-D-13-0104.1, 2013.

Liu D., G. Wang R. Mei Z. Yu, and Yu M.: Impact of soil moisture initial conditions anomalies on climate mean and extremes over Asia, J. Geophys. Res. Atmos., 119, 529–545, doi:10.1002/2013JD020890, 2014.

Loveland, T. R., Reed, B. C., Brown, J. F., Ohlen, D. O., Zhu, J., Yang, L., and Merchant, J. W.: Development of a global land cover characteristics database and IGBP DISCover from 1-km AVHRR Data, Int. J. Remote. Sens., 21, 1303–1330, 2000.

Mathon, V., Diedhiou, A., & Laurent, H. (2002). Relationship between easterly waves and mesoscale convective systems over the Sahel. Geophysical research letters, 29(8), 57-1.

Menéndez, C. G., Giles, J., Ruscica, R., Zaninelli, P., Coronato, T., Falco, M., ... & Li, L. (2019). Temperature variability and soil–atmosphere interaction in South America simulated by two regional climate models. Climate Dynamics, 53(5), 2919-2930.

Oglesby R. J., and Erickson III D. J.: Soil moisture and the persistence of North American drought. J. Climate, 2, 1362–1380, 1989.

Oglesby R. J., Marshall S., Erickson III D. J., Roads J. O. and Robertson F. R.: Thresholds in atmosphere-soil moisture interactions: Results from climate model studies. J. Geophys. Res.,107, 4244, doi:10.1029/2001JD001045, 2002.

Oleson K., Lawrence D. M., Bonan G. B., Drewniak B., Huang M., Koven C. D., Yang Z. -L.: Technical description of version 4.5 of the Community Land Model (CLM) (No. NCAR/TN-503+STR). doi:10.5065/D6RR1W7M, 2013.

Paeth H., Girmes R., Menz G. and Hense A.: Improving seasonal forecasting in the low latitudes, Mon. Weather Rev., 134, 1859-1879, 2006.

Pal J. S., Small E. E. and Elthair E. A.: Simulation of regional scale water and energy budgets: representation of subgrid cloud and precipitation processes within RegCM, J. Geophys. Res., 105, 29579–29594, 2000.

Pal J. S. and Eltahir E. A. B.: Pathways relating soil moisture conditions to future summer rainfall within a model of the land–atmosphere system. J. Climate, 14, 1227–1242, 2001.

Peterson T. C., Folland C., Gruza G., Hogg W. Mokssit A., Plummer N.: Report on the activities of the working group on climate change detection and related rapporteurs 1998-2001. Geneva (Switzerland): WMO Rep. WCDMP 47, WMO-TD 1071, 2001.

Nicholson S. E.: The West African Sahel: a review of recent studies on the rainfall regime and its interannual variability, Meteorology, 453521, 32 p., https://doi.org/10.1155/2013/453521, 2013.

Nikulin G., Jones C., Samuelsson P., Giorgi F., Asrar G., Büchner M., Cerezo-Mota R., Christensen O. B., Déque M., Fernandez J., Hansler A., van Meijgaard E., Sylla M. B. and Sushama L.: Precipitation climatology in an ensemble of CORDEX-Africa regional climate simulations, J. Climate, 6057–6078, https://doi.org/10.1175/JCLI-D-11-00375.1, 2012.

Rasmusson E. M. and Carpenter T. H.: Variations in Tropical Sea Surface Temperature and Surface Wind Fields Associated with the Southern Oscillation/El Niño. Mon. Weather Rev. 110, 354, 1982.

Reynolds, R. W. and Smith, T. M.: Improved global sea surface temperature analysis using optimum interpolation, J. Climate, 7, 929–948, 1994.

630 Seager R., and Vecchi G. A.: Greenhouse warming and the 21st century hydroclimate of
631 southwestern North America. Proc. Natl. Acad. Sci. USA, 107, 21 277–21 282,
632 doi:10.1073/pnas.0910856107, 2010.

633

634 Simmons A. S., Uppala D. D. and Kobayashi S.: ERA-interim: new ECMWF reanalysis products
635 from 1989 onwards, ECMWF Newsl., 110, 29–35, 2007.

636

637 Solmon F., Giorgi F., and Liousse C.: Aerosol modeling for regional climate studies: application
638 to anthropogenic particles and evaluation over a European/African domain, Tellus B, 58, 51–72,
639 2006.

640

641 Sundqvist H. E., Berge E., and Kristjansson J. E.: The effects of domain choice on summer
642 precipitation simulation and sensitivity in a regional climate model, J. Climate, 11, 2698-2712,
643 1989.

644

645 Takahashi, H. G., & Polcher, J. (2019). Weakening of rainfall intensity on wet soils over the wet
646 Asian monsoon region using a high-resolution regional climate model. Progress in Earth and
647 Planetary Science, 6(1), 1-18.

648

649 Thorncroft, C. D. and Blackburn, M.: Maintenance of the African easterly jet, Q. J. R. Meteorol
650 Soc., 125, 763–786, 1999.

651

652 Uppala S., Dee D., Kobayashi S., Berrisford P. and Simmons A.: Towards a climate data
653 assimilation system: status update of ERA-interim, ECMWF Newsl., 15, 12–18, 2008.

654

655 Vinnikov K. Y. and Yeserkepova I. B.: Soil moisture: Empirical data and model results, J. Clim.,
656 4(1), 66–79, doi:10.1175/1520-0442(1991) 004<0066:SMEDAM>2.0.CO;2, 1991.

657

658 Vinnikov K. Y., Robock A., Speranskaya N. A. and Schlosser A.: Scales of temporal and spatial
659 variability of midlatitude soil moisture, J. Geophys. Res., 101(D3), 7163–7174,
660 doi:10.1029/95JD02753, 1996.

661

Wang, G., Yu, M., Pal, J. S., Mei, R., Bonan, G. B., Levis, S., and Thornton, P. E.: On the development of a coupled regional climate vegetation model RCM-CLM-CN-DV and its validation its tropical Africa, Clim. Dynam, 46, 515–539, 2016.

Xue Y., De Sales F., Lau K. M. W., Bonne A., Feng J., Dirmeyer P., Guo Z., Kim K. M., Kitoh A., Kumar V., Poccard-Leclercq I., Mahowald N., Moufouma-Okia W., Pegion P., Rowell D. P., Schemm J., Schulbert S., Sealy A., Thiaw W. M., Vintzileos A., Williams S. F. and Wu M. L.: Intercomparison of West African Monsoon and its variability in the West African Monsoon Modelling Evaluation Project (WAMME) first model Intercomparison experiment, Clim. Dynam., 35, 3–27, https://doi.org/10.1007/s00382-010-0778-2, 2010.

Zakey A. S., Solmon F., and Giorgi F.: Implementation and testing of a desert dust module in a regional climate model, Atmos. Chem. Phys., 6, 4687–4704, https://doi.org/10.5194/acp-6-4687-2006, 2006.

Zeng X., Zhao M. and Dickinson R .E.: Intercomparison of bulk aerodynamic algorithms for the computation of sea surface fluxes using TOGA COARE and TAO DATA, J. Climate, 11, 2628-2644, 1998.

Zhang, J., W.-C. Wang, and J. Wei, Assessing land-atmosphere coupling using soil moisture from the Global Land Data Assimilation System and observational precipitation, J. Geophys. Res., 113, D17119, doi:10.1029/2008JD009807, 2008.

Zhang, J., W.-C. Wang, and L. R. Leung.: Contribution of land-atmosphere coupling to summer climate variability over the contiguous United States, J. Geophys. Res., 113, D22109, doi:10.1029/2008JD010136, 2008.

Zhang, J. Y., L. Y. Wu, and W. Dong,: Land-atmosphere coupling and summer climate variability over East Asia, J. Geophys. Res., 116, D05117, doi 10.1029/2010JD014714, 2011.

704 **Tables and figures:**
705

	Central Sahel		West Sahel		Guinea		West Africa	
	PCC	MB (%)	PCC	MB (%)	PCC	MB (%)	PCC	MB (%)
CTRL_2003	0.98	−47.97	0.87	−75.76	0.82	−47.12	**0.73**	**−49.31**
CTRL_2004	0.98	−47.89	0.87	−68.35	0.85	−51.97	**0.77**	**−50.56**

706

707 **Table1:** The pattern correlation coefficient (PCC) and the mean bias (MB) for JJAS precipitation
708 for model simulations with respect to CHIRPS, calculated for Guinea coast, central Sahel, west
709 Sahel and the entire West African domain during the period 2003 and 2004.

		Central Sahel		West Sahel		Guinea coast		West Africa	
		ΔWC	ΔDC	ΔWC	ΔDC	ΔWC	ΔDC	ΔWC	ΔDC
Precipitation (%)	2003	13.80	−**4.09**	29.95	6.58	19.40	9.20	8.88	4.68
	2004	15.86	−3.29	**38.58**	−1.25	26.6	12.68	10.72	7.64
Temperature mean (°C)	2003	−1.48	**0.56**	−**1.55**	−0.41	−0.15	0.54	−0.62	0.50
	2004	−**1.51**	0.47	−1.15	−0.24	−0.19	**0.59**	−0.41	0.59
Sensible heat (w.m⁻²)	2003	−16.89	8.57	−**39.66**	5.31	−2.41	7.52	−14.32	8.06
	2004	−19.53	7.55	−31.97	7.23	−3.01	**9.18**	−14.46	6.81
Latent heat (w.m⁻²)	2003	21.27	−6.67	34.21	-6.06	3.09	−13.38	15.86	−8.07
	2004	28.55	−4.81	**36.49**	-6.20	7.09	−**14.64**	19.68	−8.53
PBL (m)	2003	−233.49	81.23	−**293.23**	−0.16	−94.42	132.74	−128.90	75.57
	2004	−223.06	49.48	−247.08	19.87	−119.38	**146.80**	−117.69	56.53

725

726   **Table2:** Table summarizing the maximum values of change obtained from the PDF distribution

727   for precipitation, temperature, sensible heat, latent heat and PBL, calculated for Guinea coast,

728   central Sahel, west Sahel and the entire West African domain during the period JJAS 2003 and

729   JJAS 2004.

730

731

732

733

	Central Sahel		West Sahel		Guinea		West Africa	
	PCC	MB (°C)	PCC	MB (°C)	PCC	MB (°C)	PCC	MB (°C)
CTRL_2003	0.99	1.52	0.99	2.68	0.99	−0.34	0.99	0.85
CTRL_2004	0.99	1.50	0.99	2.14	0.99	−0.57	0.99	0.51

734

735   **Table3:** The pattern correlation coefficient (PCC) and the mean bias (MB) for JJAS 2m-

736   temperature for model simulations with respect to CRU, calculated for Guinea coast, central

737   Sahel, west Sahel and the entire West African domain during the period JJAS 2003 and JJAS

738   2004.

739

740

741

742

743

744

745
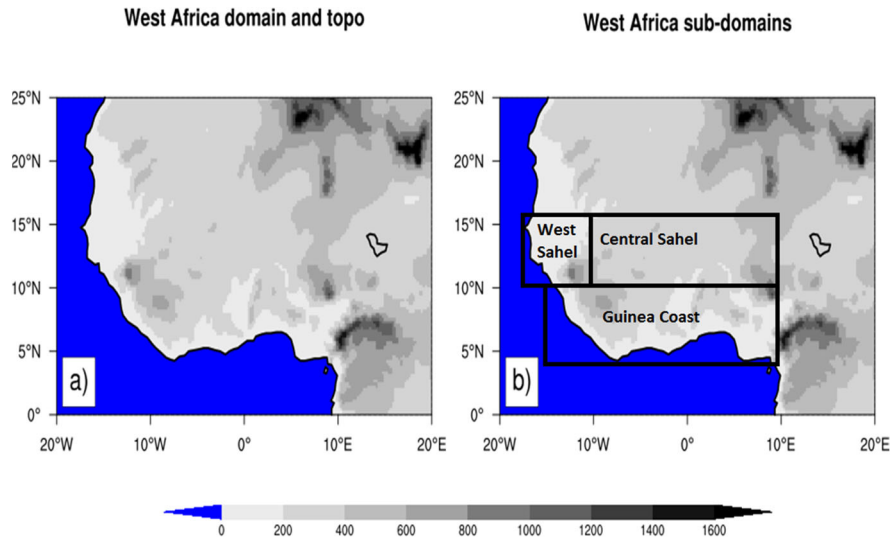
Figure 1: Topography of the West African domain. The analysis of the model result has an emphasis on the whole West African domain and the three sub-regions Guinea coast, central Sahel and west Sahel, which are marked with black boxes.

751

752

753

754

755

756

757

758

759

760

761

762

763

764

765

766

767

768

769

770

771

772
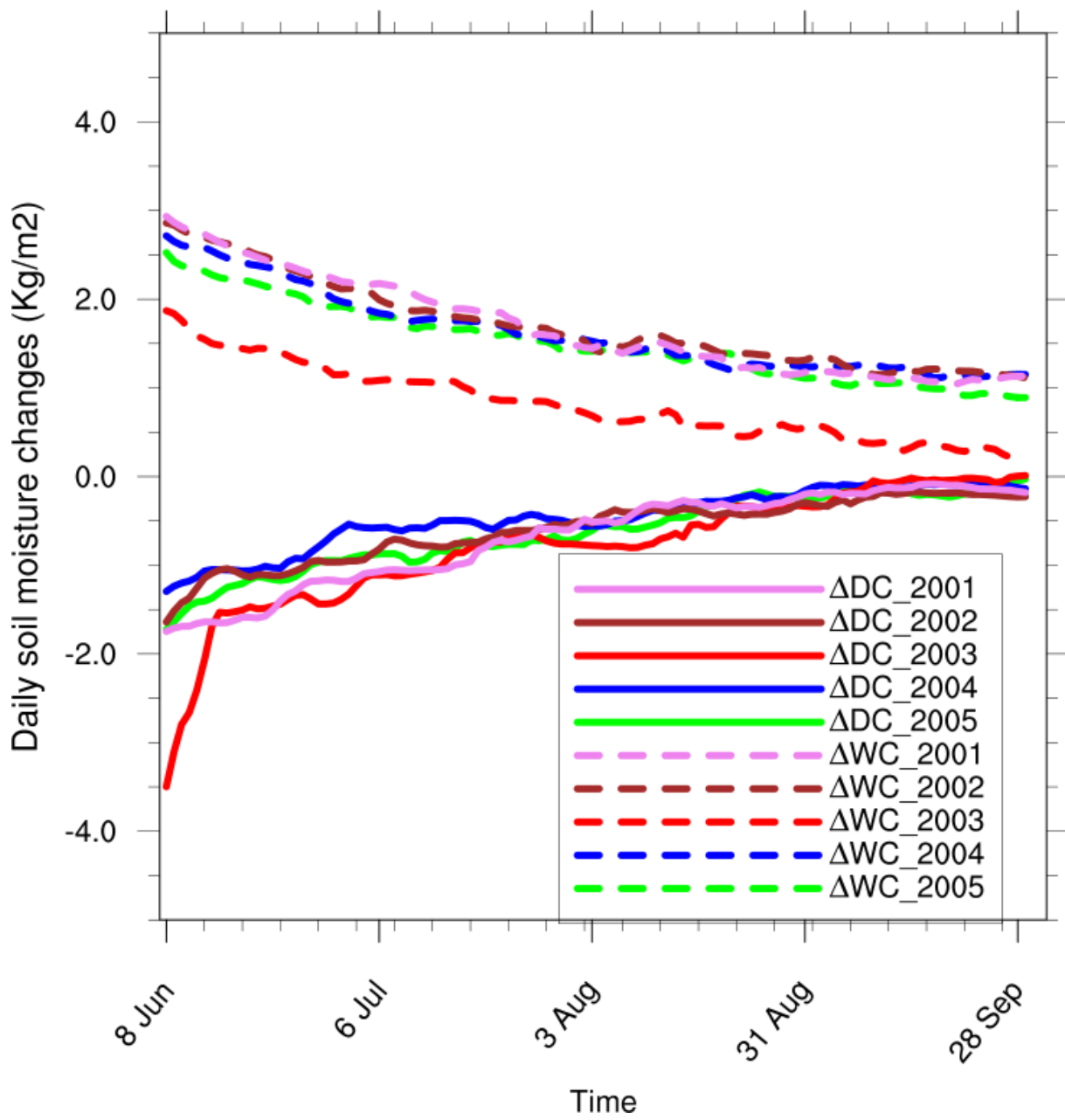
Figure 2: Changes in daily soil moisture in the 5 runs (JJAS 2001 to 2005) over West African domain, for the dry (ΔDC) and wet (ΔWC) experiments with respect to their corresponding control experiment.
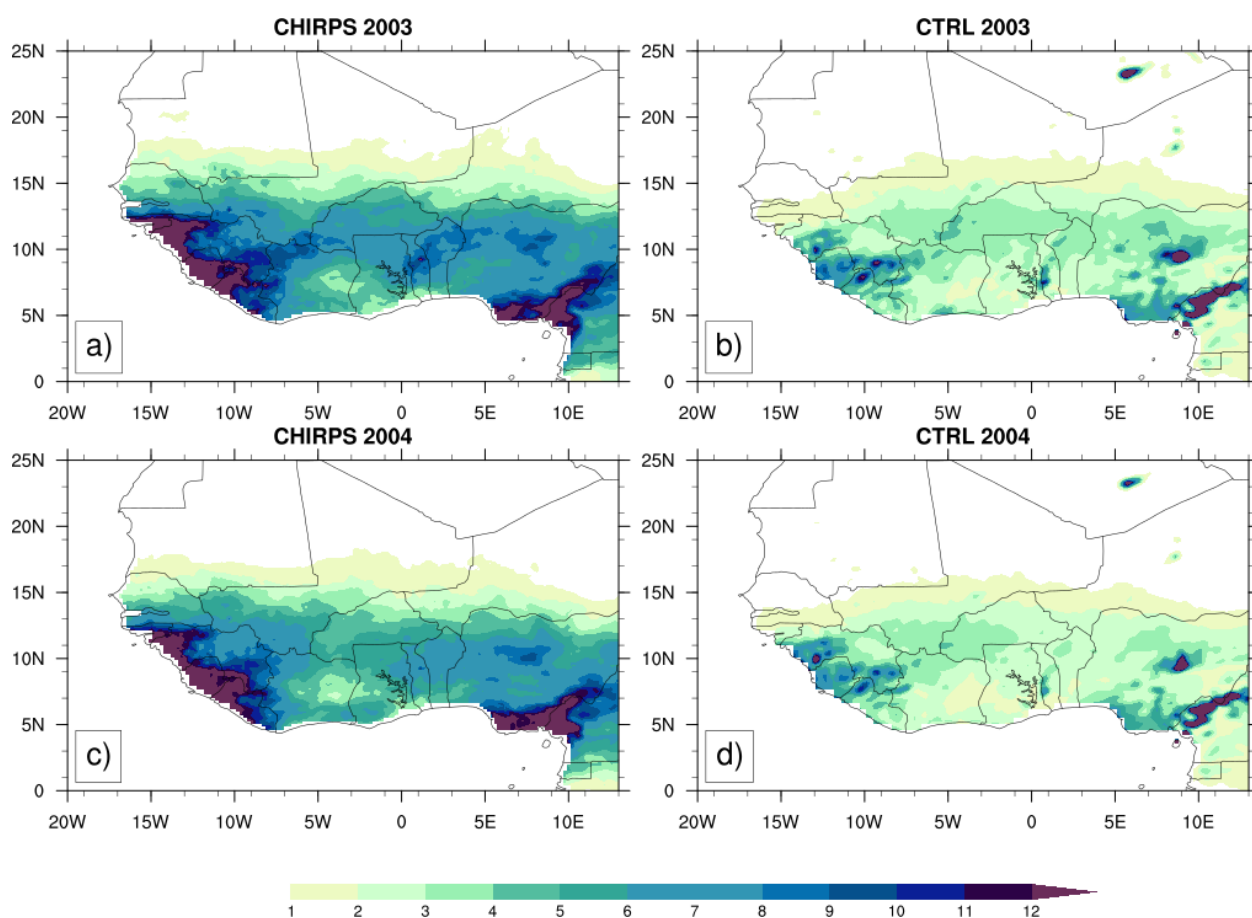
Figure3: Mean precipitation (mm/day) from CHIRPS (a, c) and the simulated control experiments (CTRL) (b, d) with the reanalysis initial soil moisture ERA20C during JJAS 2003 and JJAS 2004.

791

792

793

794

795

796

797

798

799

800
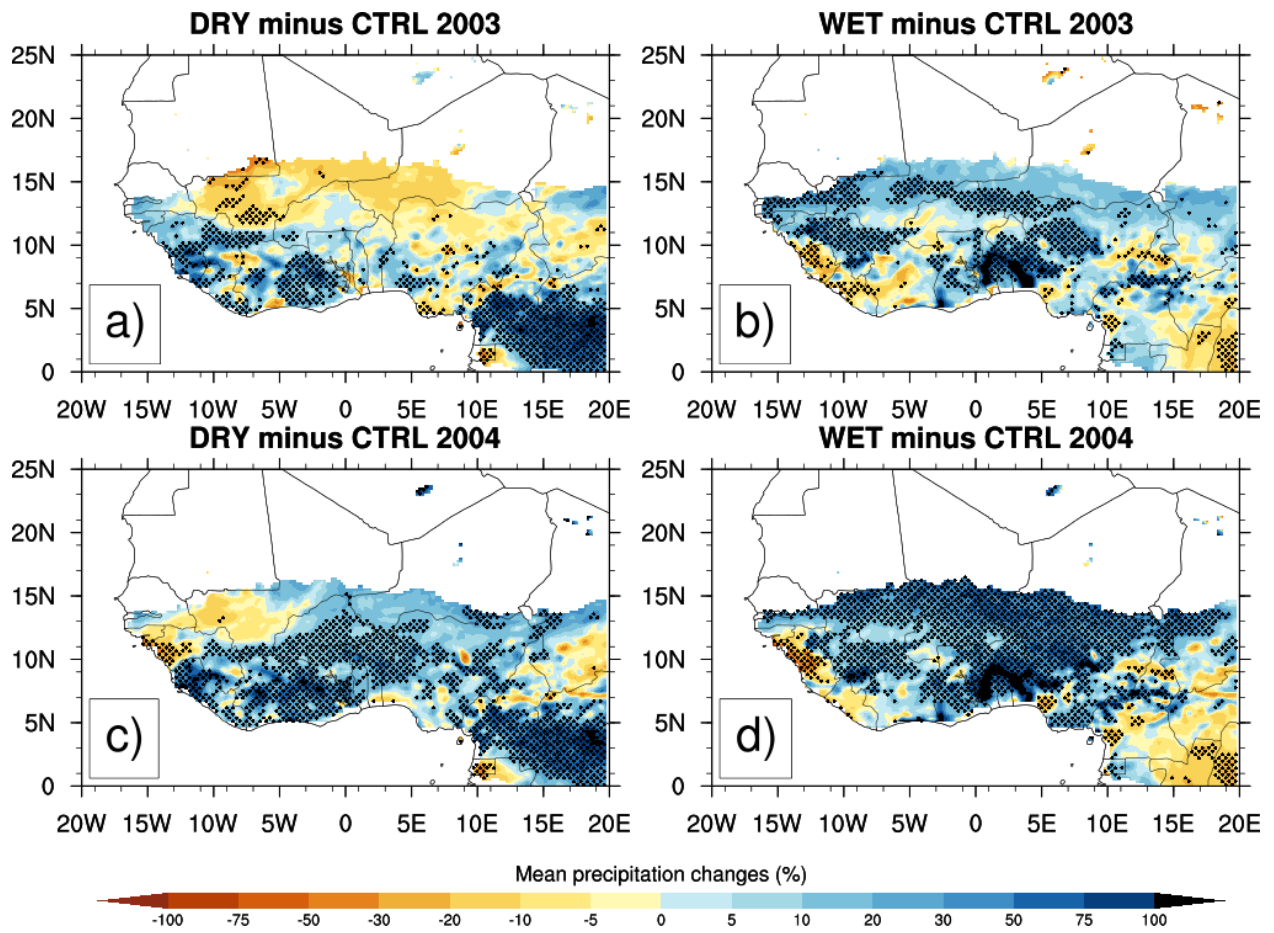
Figure4: Changes in mean precipitation (in %) for JJAS 2003 and JJAS 2004, from dry (resp. a and c) and wet (resp. b and d) experiments with respect to the control experiment, the dotted area shows differences that are statistically significant at 0.05 level.

804

805

806

807

808

809

810

811

812

813

814

815

816

817

818

830

Figure 6: Daily domain-average soil moisture changes for JJAS 2003 and JJAS 2004, from dry (ΔDC) and wet (ΔWC) experiments with respect to the control experiment.

844 **Figure 7:** Daily domain-average precipitation changes for JJAS 2003 and JJAS 2004, from dry

845 (ΔDC) and wet (ΔWC) experiments with respect to the control experiment.

846

847

848

849

850

851

852
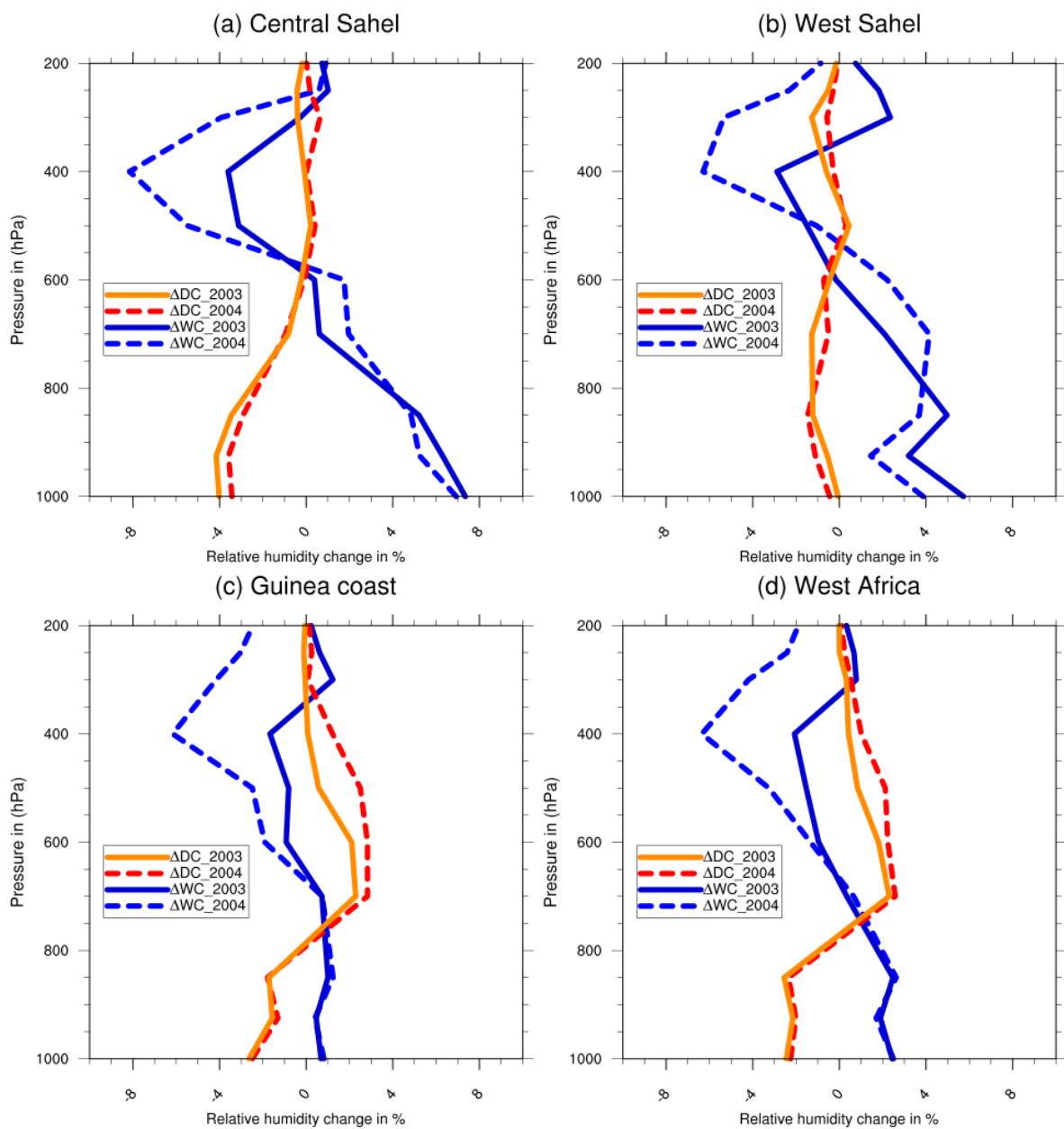
853

854

855

856 **Figure 8:** Vertical profile changes in Relative humidity for JJAS 2003 and JJAS 2004 from the

857 dry (ΔDC) and wet (ΔWC) experiments with respect to corresponding control experiment over

858 (a) central Sahel, (b) west Sahel, (c) Guinea coast, and (d) West Africa.

859

860
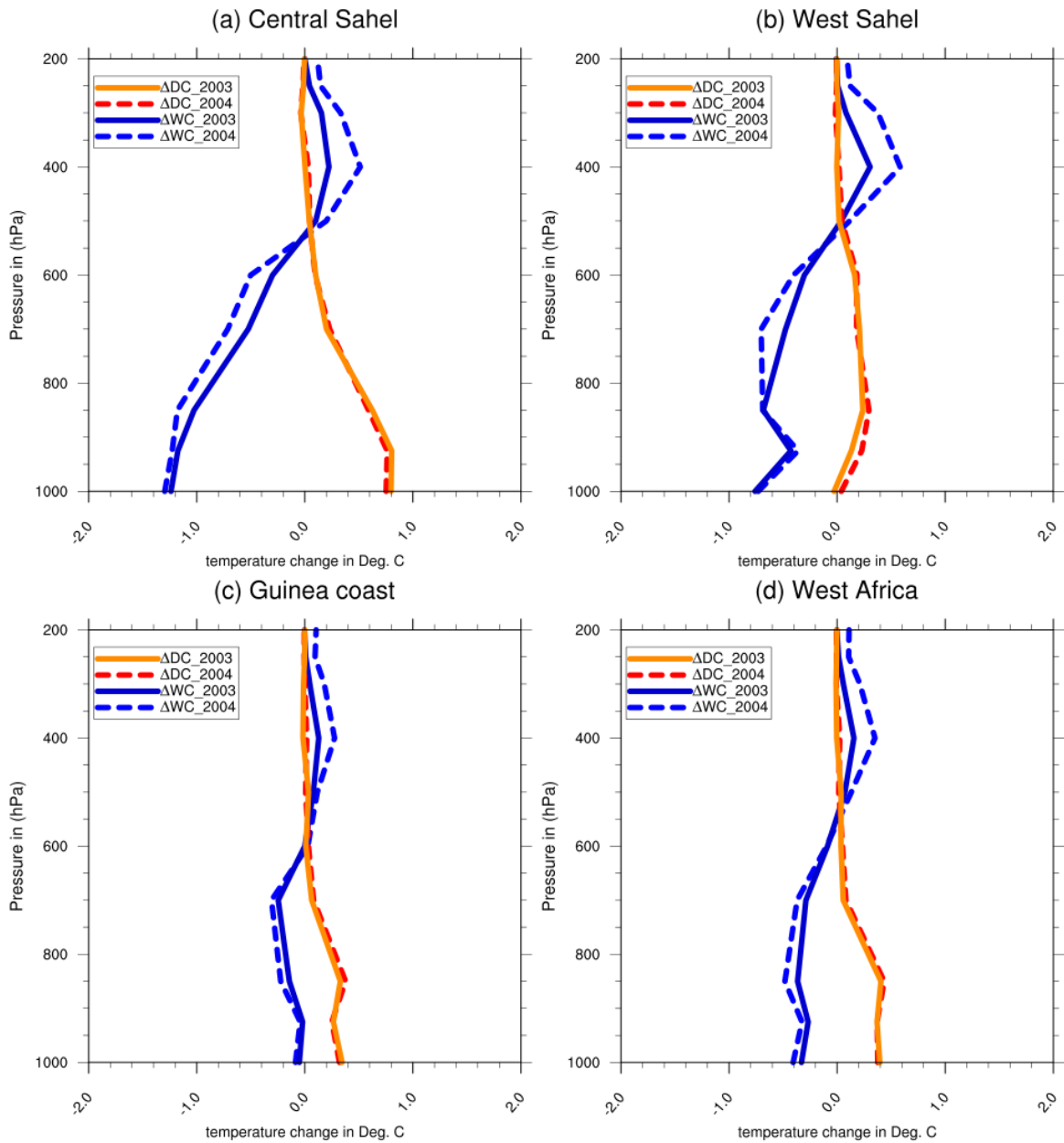
861

862 **Figure 9:** Vertical profile changes in temperature for JJAS 2003 and JJAS 2004 from the dry

863 (ΔDC) and wet (ΔWC) experiments with respect to the control experiment over (a) central Sahel,

864 (b) west Sahel, (c) Guinea coast, and (d) West Africa.

865

866
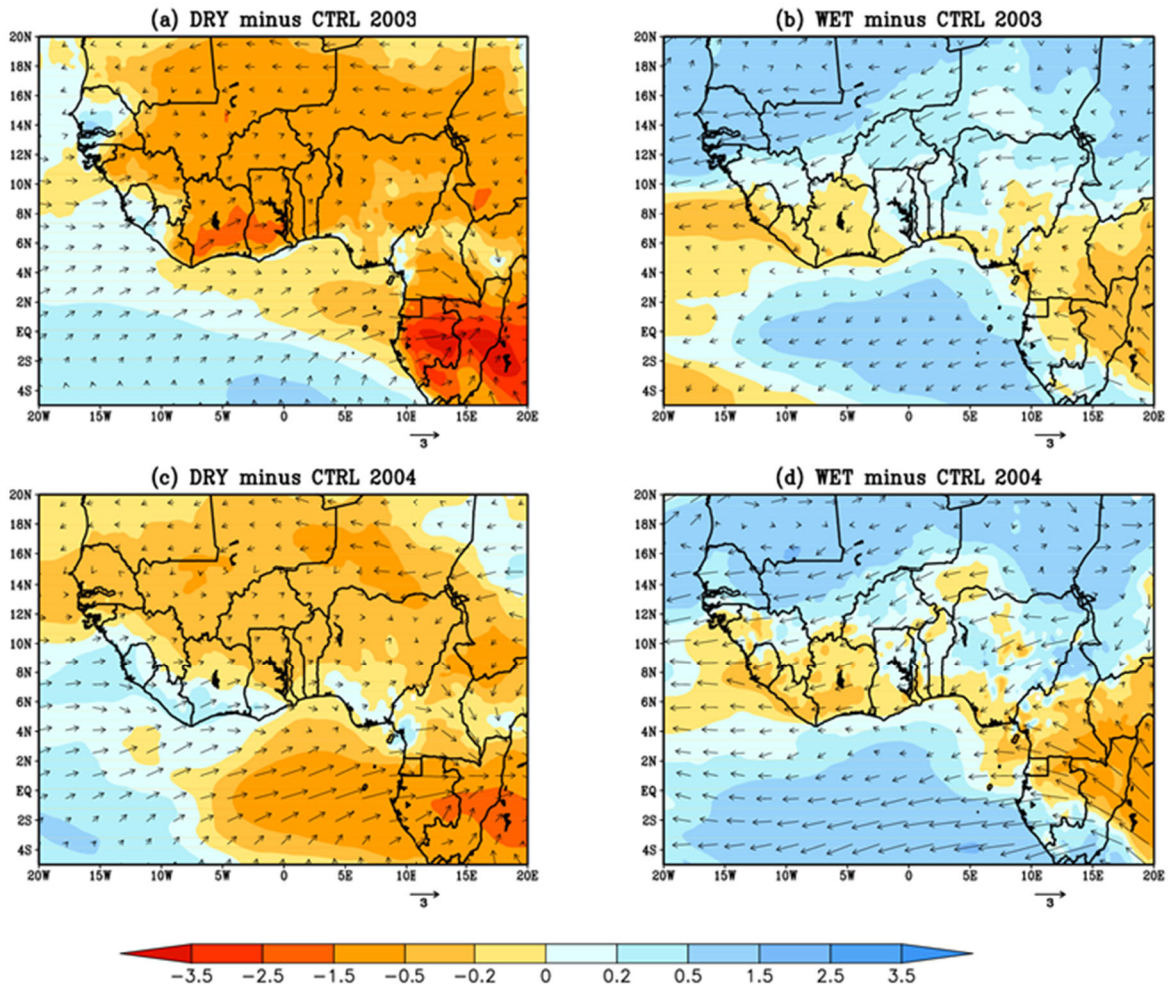
Figure 10: The lower tropospheric wind (850hpa) and moisture bias for JJAS 2003 and JJAS 2004 from the dry (a and c) and wet (b and d) experiments with respect to the control experiment.

884

885

886
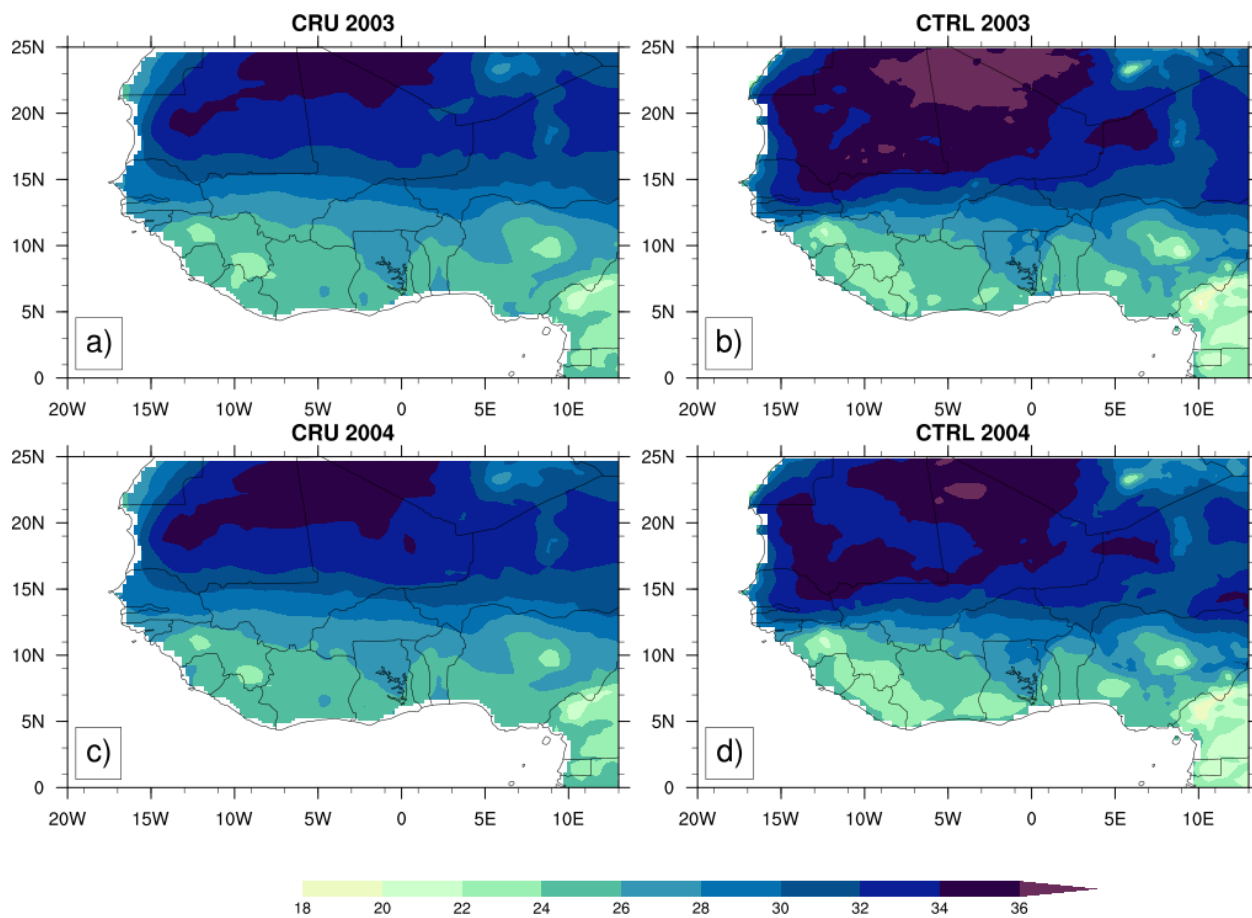
Figure 11: Mean 2m-temperature (°C) from CRU (a and c) for JJAS 2003 and JJAS 2004 and

the simulated control experiment (b and d) with the reanalysis initial soil moisture ERA20C.

889

890

891

892

893

894

895

896

897

898

899

900

901

902

903

904

905

Figure 12: Changes in 2m-temperature (°C) for JJAS 2003 and JJAS 2004, from dry (resp. a and c) and wet (resp. b and d) experiments with respect to the control experiment, the dotted area shows differences that are statistically significant at 0.05 level.
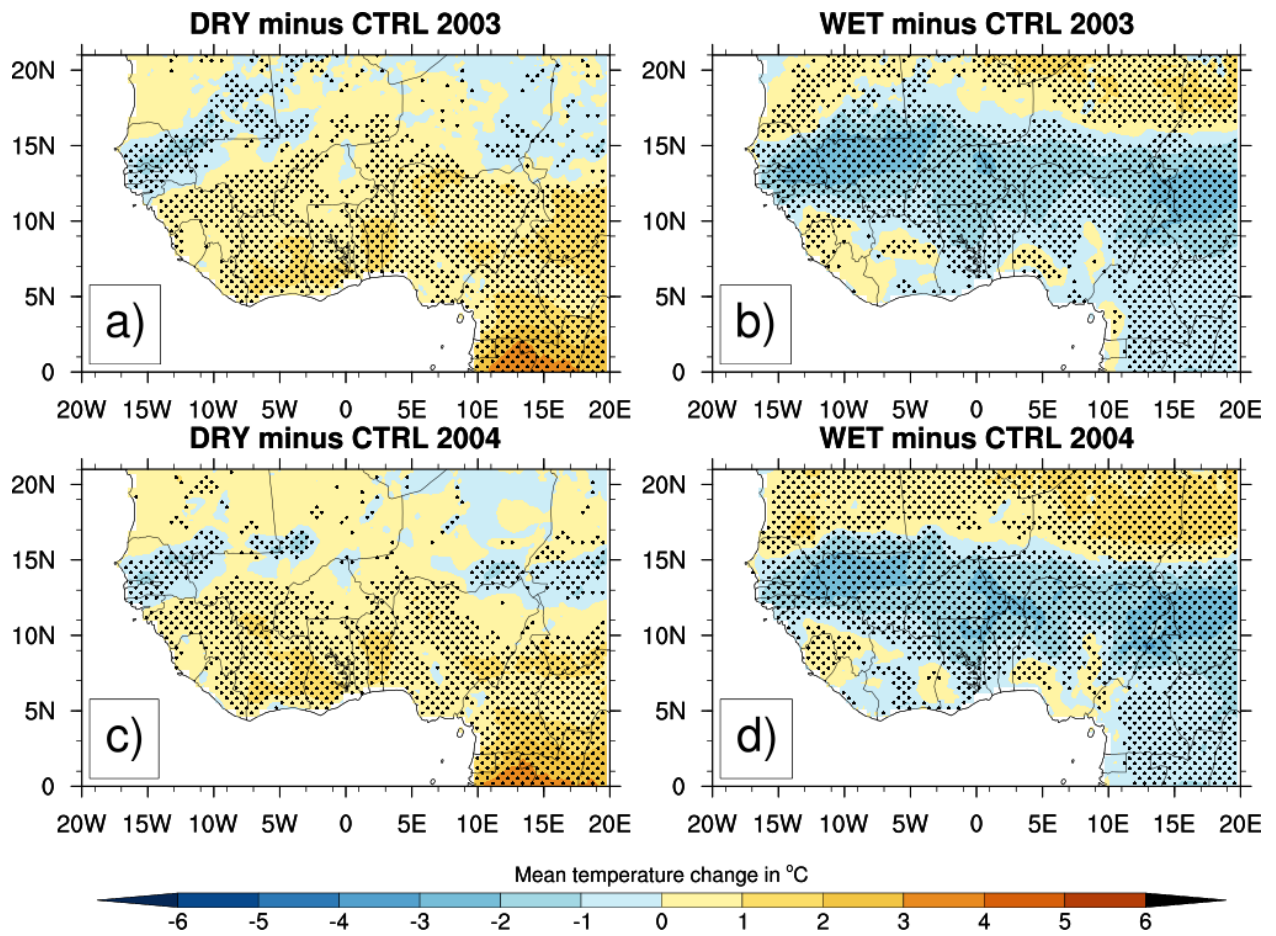
909

910

911

912

913

914

915

916

917

918

919

920

921
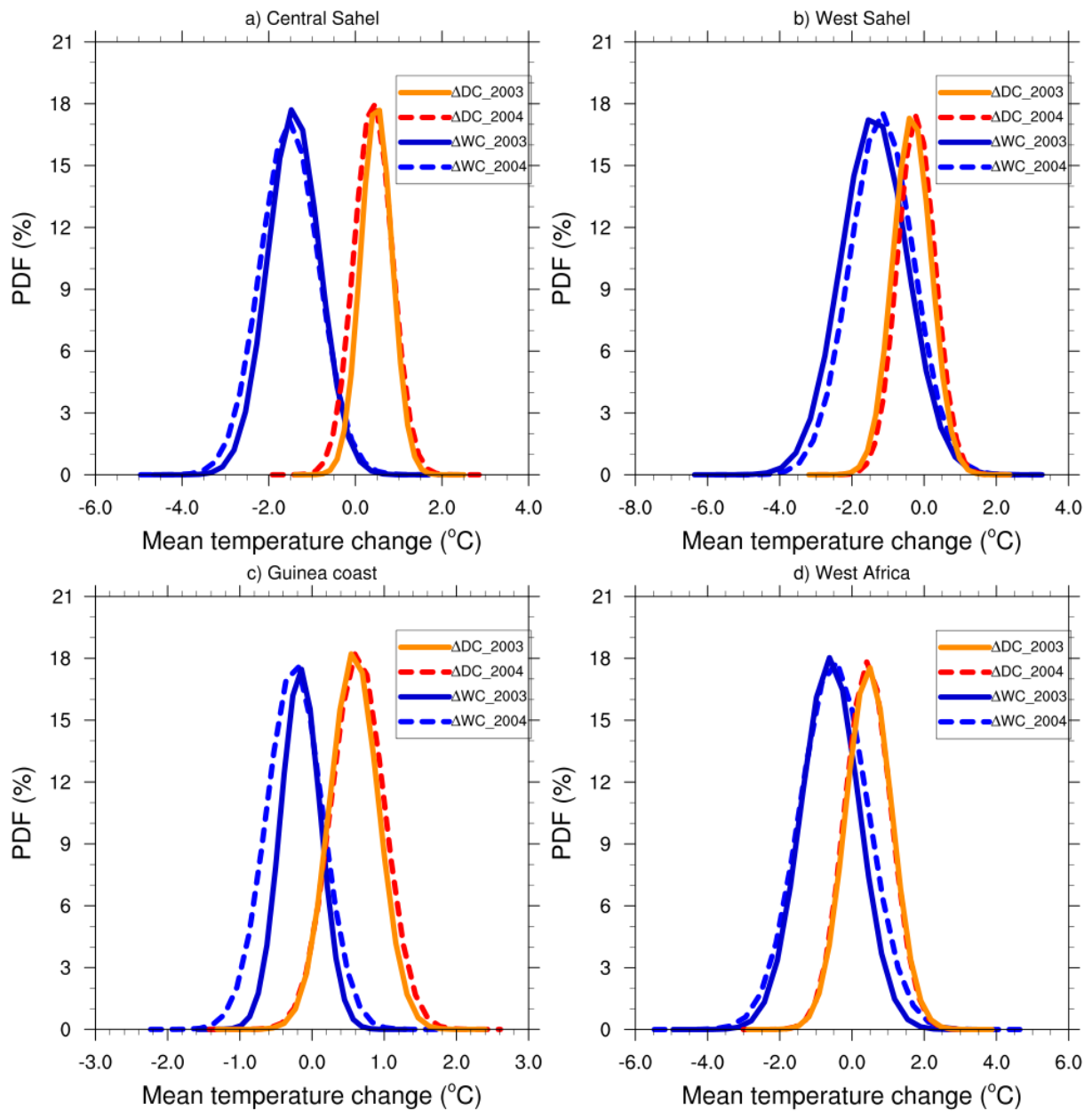
Figure 13: PDF distributions (%) of mean temperature changes in JJAS 2003 and JJAS 2004, over (a) central Sahel, (b) West Sahel, (c) Guinea and (d) West Africa derived from dry (ΔDC) and wet (ΔWC) experiments compared to the control experiment.

925

926

927

928

929

930
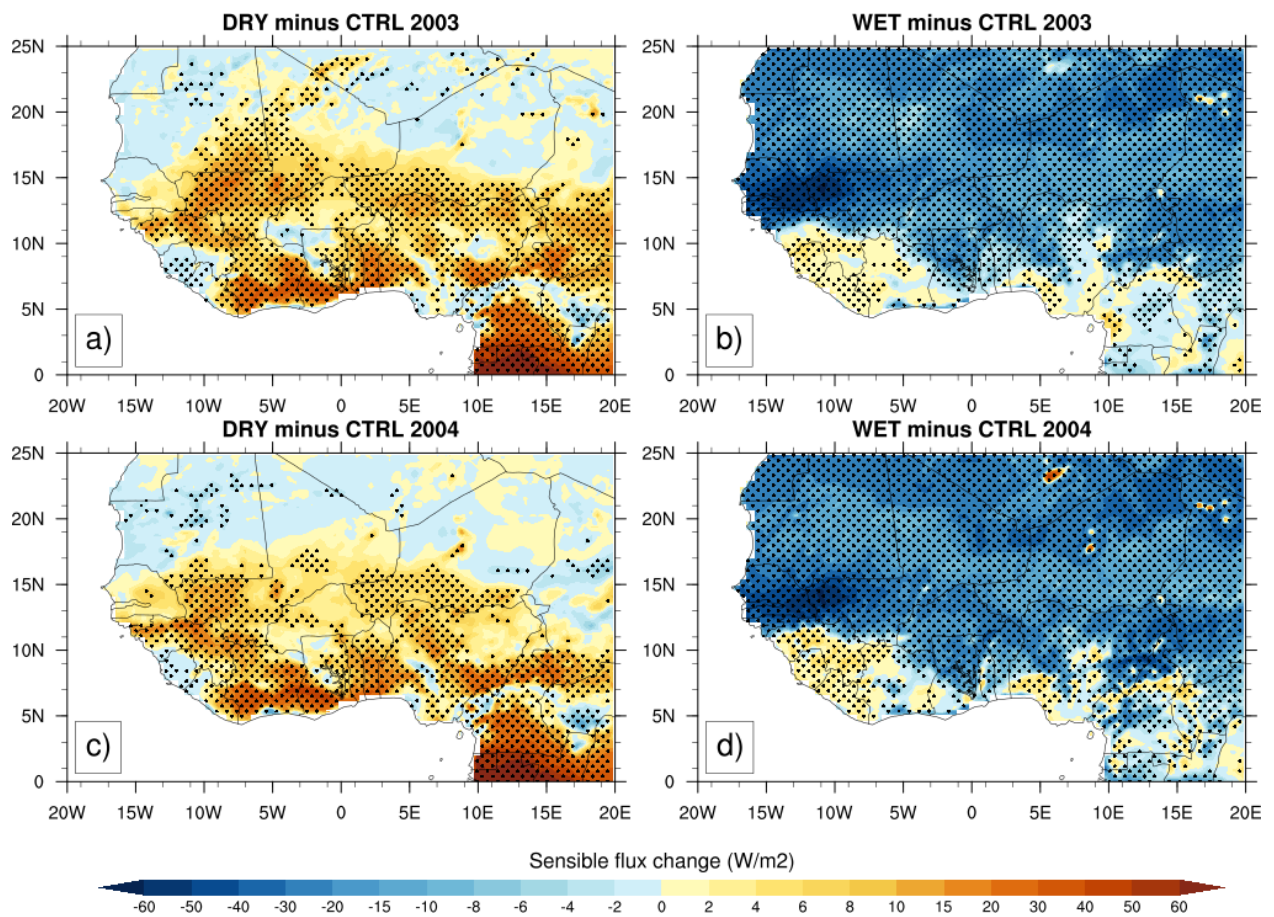
Figure 14: Same as Fig.12 but for sensible heat fluxes (in W.m^{-2}).

949

950

951
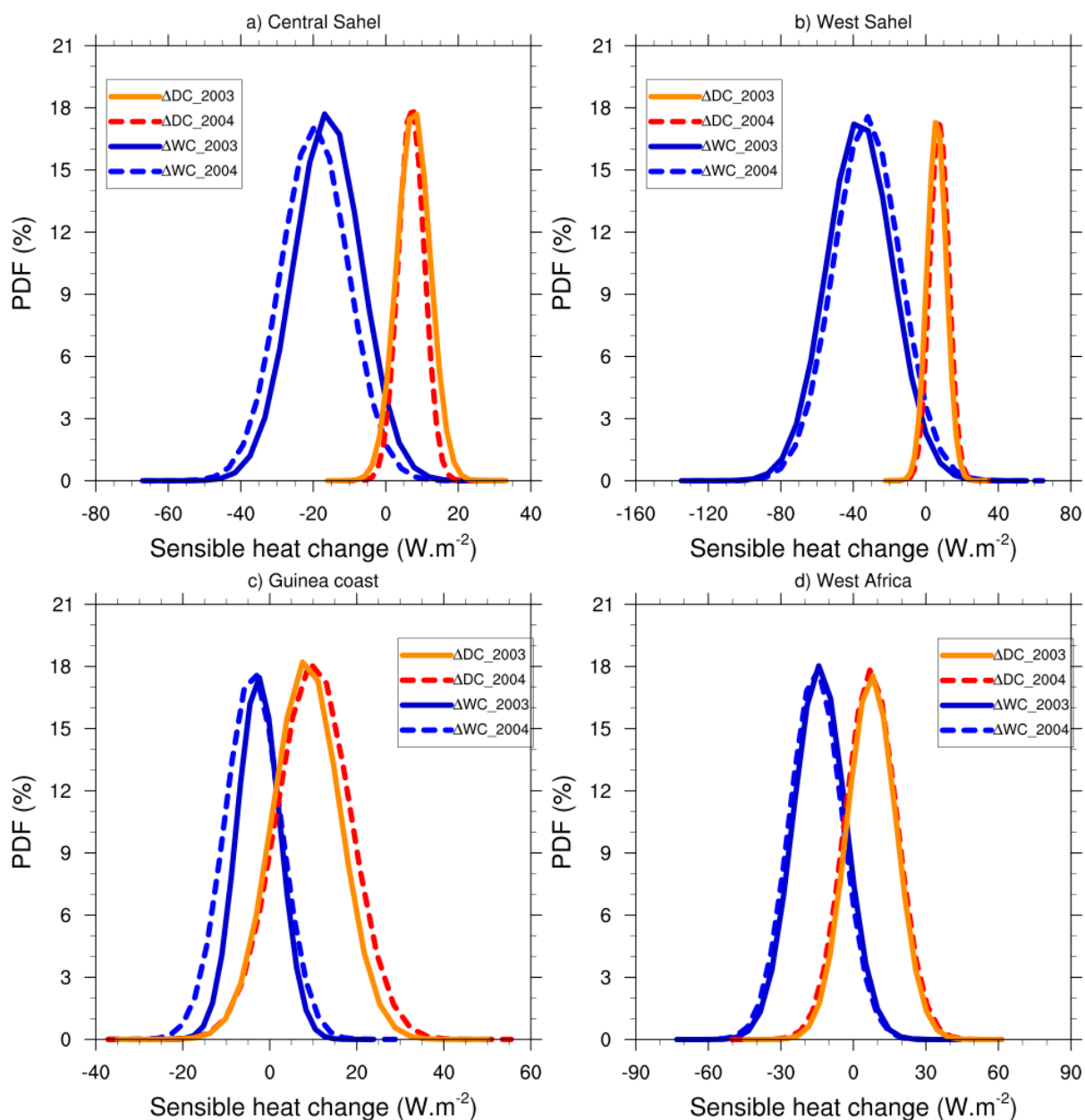
Figure 15: Same as Fig.13 but for sensible heat fluxes (in W.m^{-2}).

953

954

955

956

957

958

959

960

961

962

963
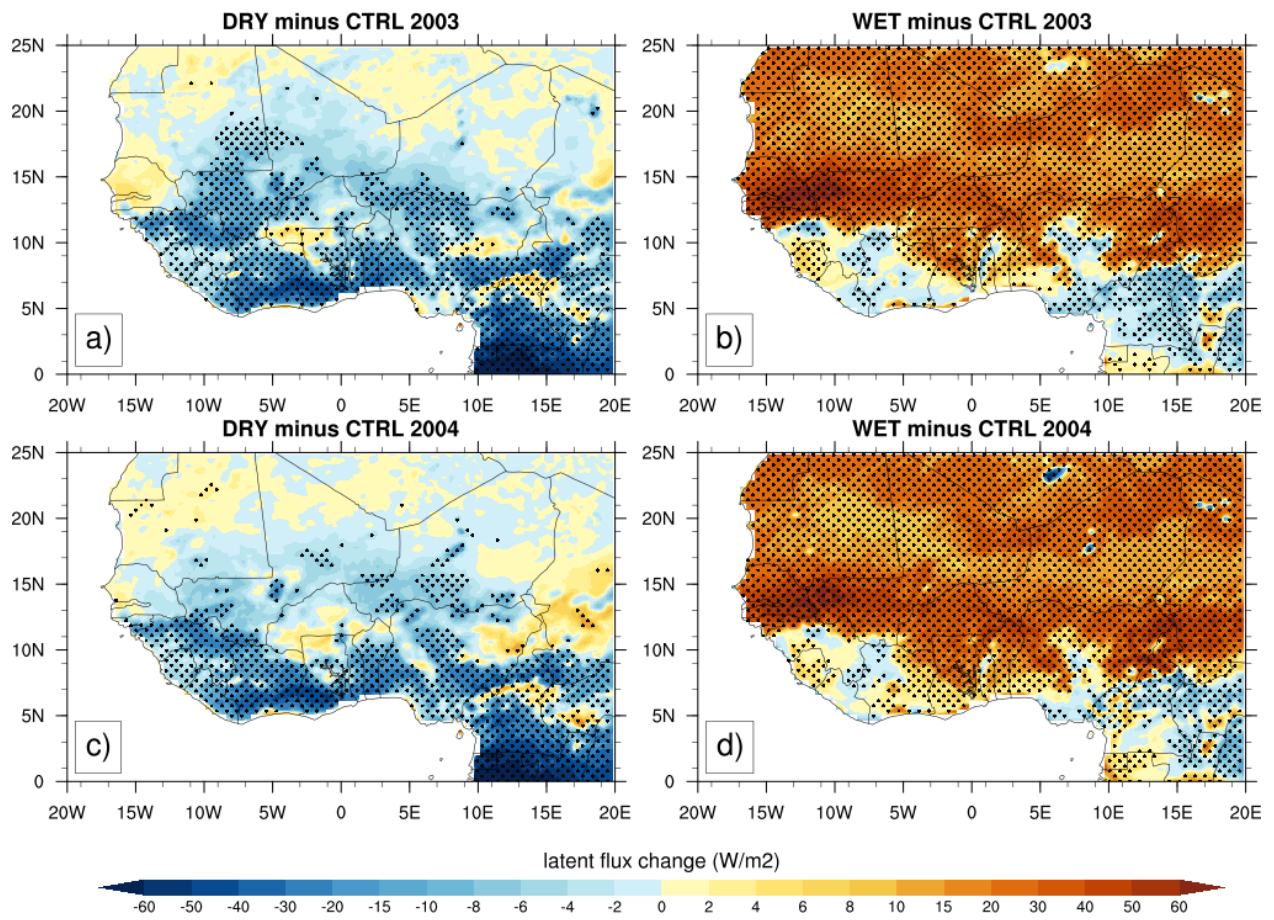
Figure 16: Same as Fig.12 but for latent heat fluxes (in W.m^{-2}).

965

966

967

968

969

970

971

972

973

974

975

976

977

978
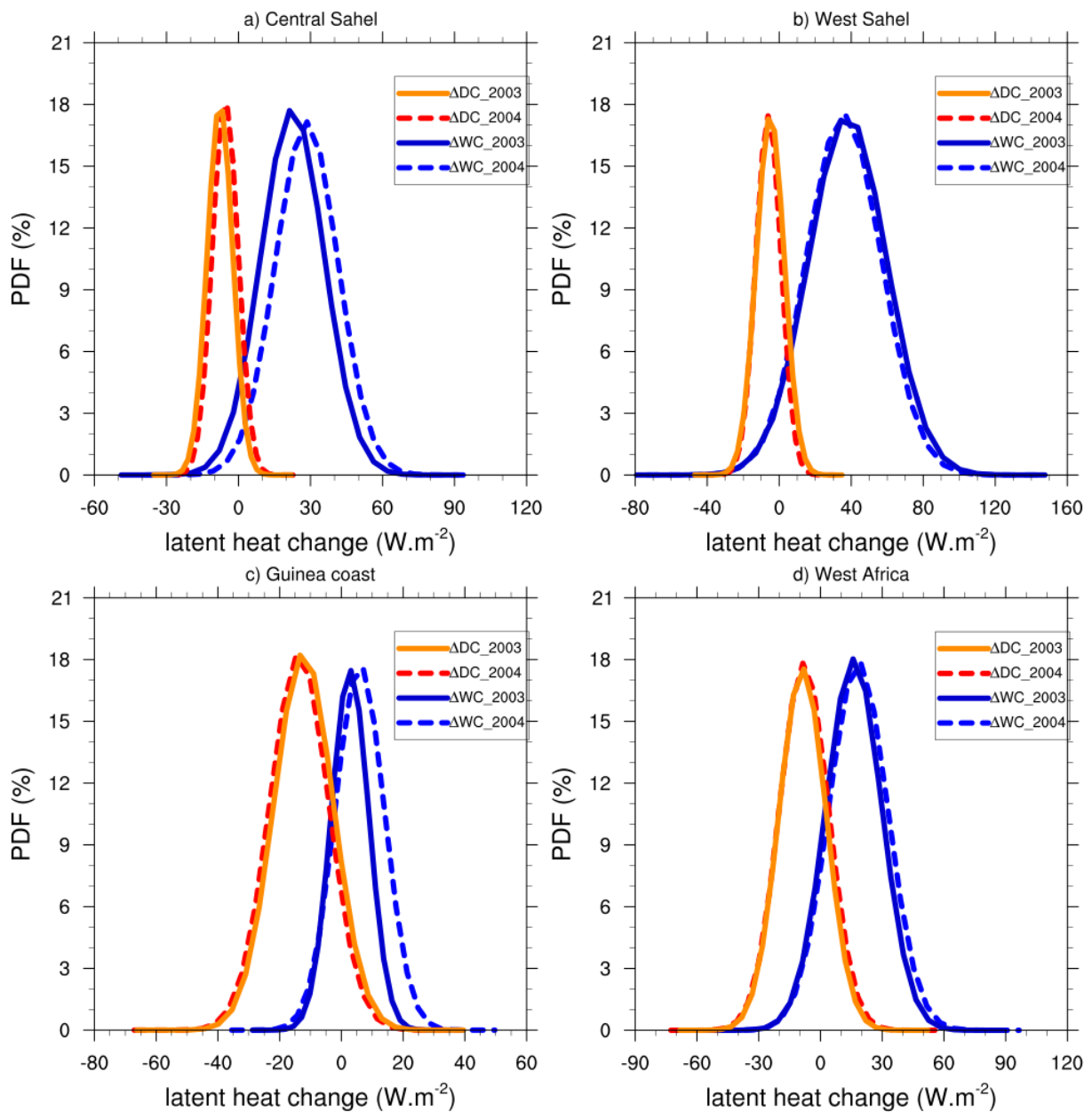
Figure 17: Same as Fig.13 but for latent heat fluxes (in W.m^{-2}).
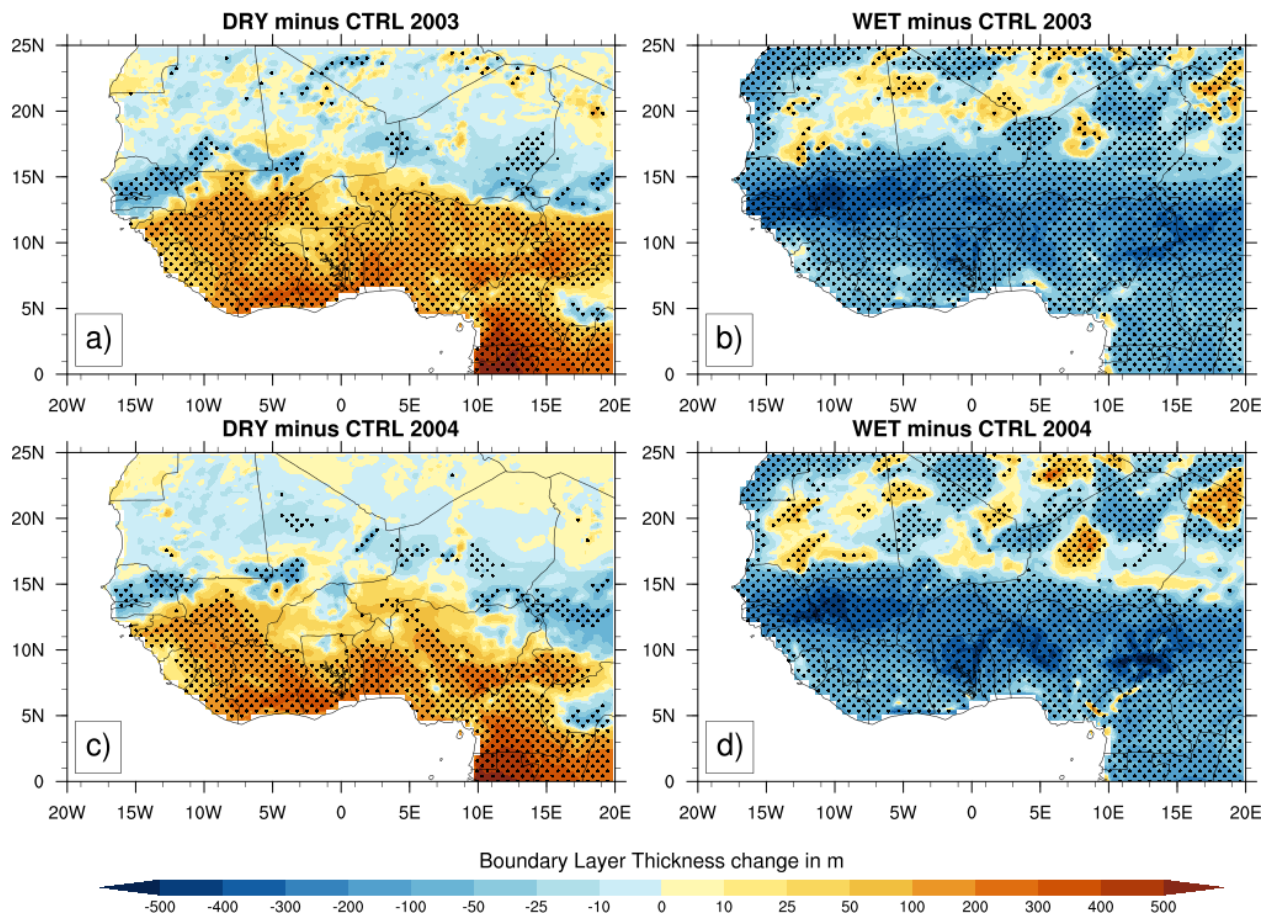
Figure 18: Same as Fig.12 but for the change of the height of the planetary boundary layer (in m).

1009
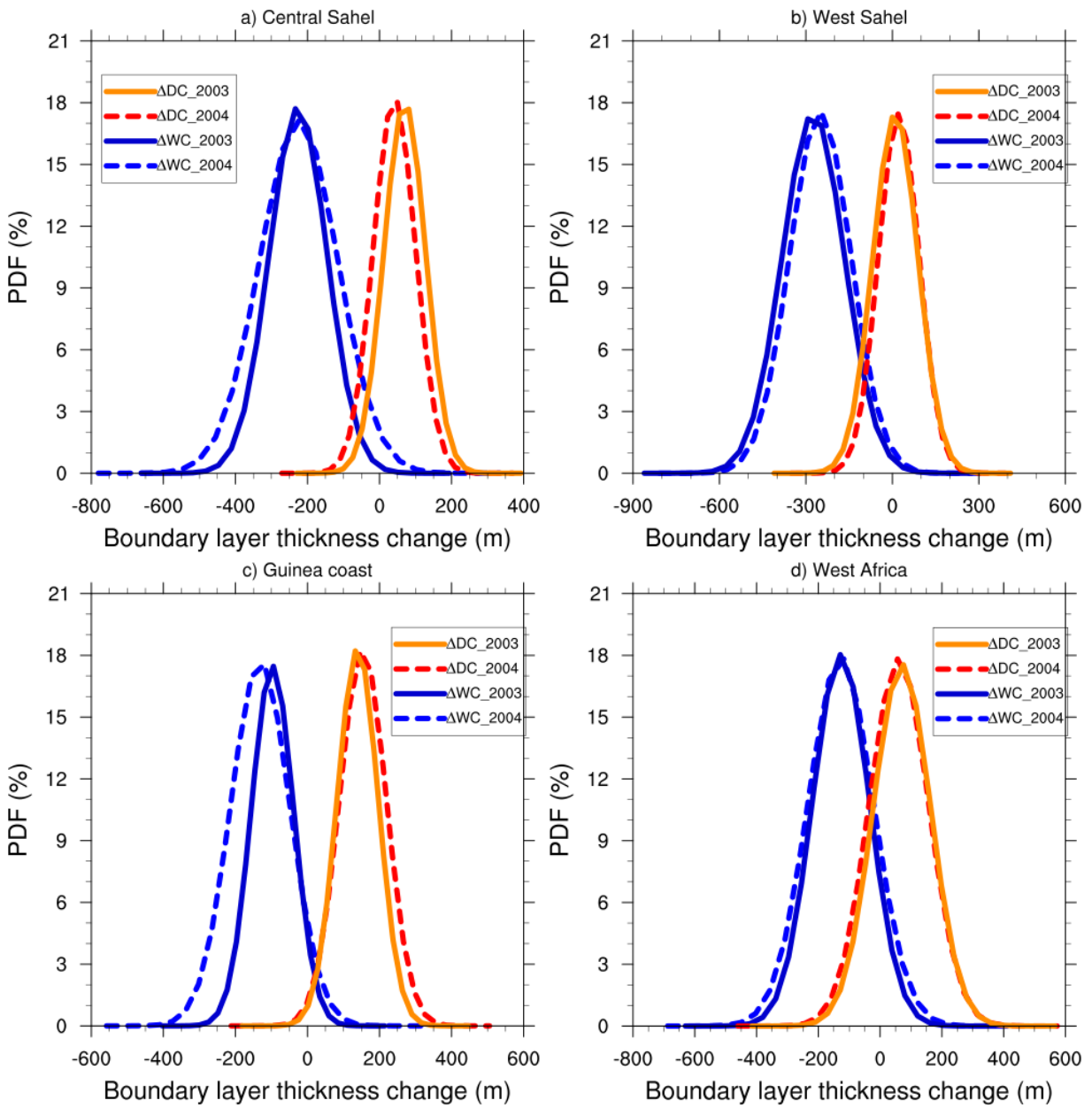
1010

1011

1012 **Figure 19:** Same as Fig.13 but for the height of the planetary boundary layer (in m).

1013

1014

1015

1016

1017

1018

1019